Clonal Interactions in Barrett's Carcinogenesis

Sebastian Simon Zeki

Barts and The London School of Medicine and Dentistry,

Queen Mary, University of London

Primary Supervisor: Dr Stuart A C McDonald

Secondary Supervisor: Professor Nicholas A Wright

Thesis submitted for the degree of

Doctor of Philosophy at the University of London

September 2013

Abstract

Introduction:

Barrett's oesophagus (BO) is a metaplastic premalignant disease which can undergo a metaplasia-dysplasia-adenocarcinoma pathway. It represents an example of field cancerization by which an area occupied by BO can undergo molecular and genetic changes associated with carcinogenesis without being phenotypically cancerous. Previous work suggested that non-cancerous BO contains a monoclonal population. More recent work demonstrated that premalignant Barrett's fields are polyclonal suggesting that clonal interactions may be important in carcinogenesis. It is the aim of this thesis to further investigate clonal interactions in BO by understanding the effects of therapy in altering the relationships of clonal populations in BO, by assessing the relationship of clonal populations in dysplasia as compared with the associated cancer, and by attempting to elucidate a potential molecular mechanism of clonal interactions.

Results:

The overall results can be summarised as follows: 1.Premalignant clonal populations are well mixed allowing for clonal interactions. However, the adenocarcinoma associated with high grade dysplasia is monoclonal and derived from clonal populations found in the dysplasia, indicating possible

clonal interactions during carcinogenesis. 2. Patients with persistent disease after endoscopy retain the same clonal populations. However, the clonal populations of recurrent disease changes such that new clonal populations arise or may benefit from the extinction of others. 3. These clonal populations may be derived from deep submucosal glands or may be found in phenotypically normal squamous epithelium indicating a common stem cell origin. 4. A possible mechanism of clonal interaction may be the senescence associated secretory phenotype: senescence is abundant in BO and can cause proliferation in neighbouring cells in vitro.

Conclusion:

This thesis has investigated the implications of clonal interactions in BO. The demonstration of temporal clonal heterogeneity as a result of endoscopic therapy, as well as spatial clonal heterogeneity possibly resulting in carcinogenesis, asks for a mechanistic explanation of clonal interactions. The consequences of senescence may well provide one such mechanism.

Acknowledgements

Of course the first acknowledgements should go to Stuart, who buffered and weathered my endless diatribes, stream of consciousness's, growls, hilarious jokes, tics, imitations and aphorisms without so much as a whimperand Nick on whose foundations and endless ideas all our work depends on.

The lab would have been an empty shell were it not for the folk I shared bench space and the occasional outburst with. Bianca, who I hope will achieve immortality through the "quotation of the week", will be sorely missed. I hope Noor achieves the Nirvana of a dance-off in clinic, and perhaps could incorporate Annie Baker's flambé into the routine. Laura of course who has always been helpful in every way- perhaps we will pass each other on the Cambridge train someday?

Trevor Graham deserves a special mention for being ceaselessly encouraging and always novel, as well as Malcolm whose departure coincides with mine. The dinners of Joanne Chin-Aleong, probably the most generous histopathologist I've ever met, will be sorely missed.

I hope I've at least assured my funders, the Derek Butler Trust and CORE Digestive Disease Charity, that their investment was sound. Long may their work, and mine, continue.

This work was supported by CORE Digestive Diseases Charity, Grant Number: TBYG1J3R.

Disclaimer

The work presented in this thesis was based upon ideas and hypotheses generated by myself, Stuart McDonald and Nick Wright. All laboratory work was completed by myself alone.The whole genome gene expression microarray work was done at the Genome Centre, Barts Cancer Institute and help with the preliminary analysis was saught from Dr Charles Mein. Flow cytometry was carried out at the Flow cytometry core facility, Blizard Institute, Whitechapel, London with the assistance of Dr Gary Warnes. This thesis was proof read by Dr. Stuart McDonald. Professor Malcolm Alison proof read chapter 5.

The work arising from this thesis has to date led to the following original research publications:

1. Zeki SS, Haidry R, Graham TA, Rodriguez-Justo M, Novelli M, Hoare J, Dunn J, Wright NA, Lovat LB,McDonald SA. Clonal Selection and Persistence in Dysplastic Barrett's Esophagus and Intramucosal Cancers After Failed Radiofrequency Ablation.*Am J Gastroenterol. 2013 Aug 13. doi: 10.1038/ajg.2013.238.* [Epub ahead of print]

2, Khan S, McDonald SA, Wright NA, Graham TA, Odze RD, Rodriguez-Justo M, Zeki S.Crypt dysplasia in Barrett's oesophagus shows clonal identity between crypt and surface cells.*J Pathol. 2013 Sep;231(1):98-104.*

Index

Figure Index

Tables

Abbreviations

ACTB	β actin
ALA	5-aminolevulinic acid
ANOVA	Analysis of Variance
APC	Adenomatous polyposis coli
ARF	Alternative reading frame
ARID1A	AT rich interactive domain 1A
ATM	Ataxia telangiectasia mutated
ATR	ATM and Rad3-related
BDT	Big Dye Terminator
BO	Barrett's Oesophagus
BPE	Bovine pituitary extract
BSA	Bovine serum albumin
CCL5	Chemokine (C-C motif) ligand 5
CCO	Cytochrome C oxidase
CCR1	Chemokine (C-C motif) receptor
CDH1	Cadherin 1
CDK	CCR1 chemokine (C-C motif) receptor
CDKN2A	cyclin D kinase inhibitor 2A
CDX2	Caudal type homeobox2
CHK	Checkpoint kinase
CHK-2	Checkpoint kinase2 (CHK2)
CLO	Columnar Lined Oesophagus
CO2	Carbon dioxide
COSMIC	Catalogue of somatic mutations
CST3	Cystatin 3
CXCL	Chemokine (C-X-C motif) ligand 1
DAB	3,3-diaminobenzidine-tetrahydrochloride
DAPI	4',6-diamidino-2-phenylindole
DAS	Dihydroxyacetone synthase
DDR	DNA Damage Response
dlg	Discs large
DMSO	Dimethyl sulphoxide
DNA	Deoxyribonucleic Acid
DOCK2	Dedicator of cytokinesis 2
DTT	Dithiothreitol
EBI3	Epstein Barr virus induced 3
ECM	Extracellular Matrix
EDTA	Ethylenediaminetetraacetic acid
EGF	Epidermal growth factor
EGFR	Epidermal growth factor receptor
ELISA	Enzyme linked immunoabsorbent assay
ELMO1	Engulfment and cell motility protein 1
EMR	Endoscopic Mucosal Resection

ESR1	Estrogen receptor 1
FACS	Flow activated cell sorting
FBS	Foetal bovine serum
FCS	Foetal calf serum
FFPE	Formalin Fixed, Paraffin Embedded
GAPDH	Glyceraldehyde 3-phosphate dehydrogenase
GDF15	Growth differentiation factor 15
GFP	Green Fluorescent Protein
GI	Gastrointestinal
GLB1	Galactosidase β-1
GOJ	Gastro-oesophageal junction
GORD	Gastro-oesophageal reflux disease
GRO	Growth regulated oncogene
H&E	Haematoxylin and Eosin
HBEGF	Heparin binding EGF-like growth factor
HGD	High grade dysplasia
HNSCC	Head and Neck squamous cell cancer
HRP	Horse radish peroxidase
IGF	Insulin-like growth factor
IGFL1	IGF-like family member 1
IL-6/8	Interleukin 6/8
IMC	Intra mucosal cancer
ITS	Insulin-Transferrin-Sodium Selenite Supplement
JAK	Janus Kinase
KLK6	Kallikrein-related peptidase 6
LB	Luria-Bertani Broth
LCM	Laser capture microdissection
LCN2	Lipocalin-2
LGD	Low grade dysplasia
lgl	lethal-giant larvae gene
LGR5	Leucine-rich repeat-containing G-protein coupled receptor 5
LOH	Loss of heterozygosity
LTR	Long terminal repeat
MCS	Metaplasia carcinoma sequence
MDC	Metaplasia dysplasia carcinoma
MDCM	Metaplasia dysplasia carcinoma metastasis
MDM2	Murine double minute 2
MIB	E3 ubiquitin-protein ligase
MMP	Matrix metalloprotein
MoMLV-LTR	Murine Moloney Leukemia Virus
MREC	Medical ethics research committee
mTHPC	m-tetrahydroxyphenyl chlorine
MTT	3-(4,5-Dimethylthiazol-2-yl)-2,5-diphenyltetrazolium bromide
MUC	Mucin
NAD	Nicotinamide adenine dicnucleotide phosphate
ND	Non dysplastic
NDBO	Non dysplastic Barrett's oesophagus

NSE	Neo squamous epithelium
NTP	Deoxyribonucleotide triphosphates
OAC	Oesophageal adenocarcinoma
OIS	Oncogene induced senescence
PBS	Phosphate buffered saline
PCR	Polymerase Chain Reaction
PDT	Photodynamic Therapy
PIK3	Phosphoinositide 3 kinase
PPI	Proton pump inhibitor
RA	Retinoic acid
RAC1	Ras-related C3 botulinum toxin substrate 1
RANTES	Chemokine (C-C motif) ligand 5
Rb	Retinoblastoma protein
RFA	Radiofrequency Ablation
RIN	RNA integrity number
RNA	Ribonucleic Acid
RPMI-1640	Roswell Park Memorial Institute media
RT	Reverse transcriptase
SA β-Galactosidase	Senescence associated β-Galactosidase
SAA1	Serum amyloid A1
SAHF	Senescence Associated Heterochromatin Foci
SASP	Senescence Associated Secretory Profile
SCJ	Squamo-columnar Junction
scrib	Scribble gene
SFN	stratifin
SM	submucosal
SMARCA4	SWI/SNF-related, Matrix-associated, Actin-dependent Regulator Chromatin
STAT	Signal Transducer And Activator Of Transcription
STRING	Search Tool for the Retrieval of Interacting Genes
TAD	Transcription-activation domain
TBE	Tris/Borate/EDTA
TERT	Telomerase Reverse Transcriptase
TFF	Trefoil factor
TGF	Transforming growth factor
TNM	Tumour-Node-Metastasis
TP53	Tumour Protein 53
UBC	Ubiquitin C
UCLH	University College London Hospital
UK	United Kingdom
USA	United States of America
UV	Ultra-violet
WAF1	Cyclin-dependent kinase inhibitor 1
Wt	Wild Type

Chapter 1 Introduction

1.1 Macroscopic and microscopic histopathology of the normal oesophagus

1.1.1 Macroscopic Histology of the normal oesophagus

The normal human oesophagus is a muscular tubular structure designed to propel food from the oropharynx to the stomach using peristalsis. It has no absorptive functions and its only secretive function is that of mucin production to lubricate the passage of food. In human adults it is around 25cm long extending from the cricopharyngeus muscle in the pharynx to the lower oesophageal sphincter at the gastroesophageal junction (GOJ).

The GOJ is defined as the proximal limit of the gastric rugal folds. Endoscopically the z-line is the line that defines the end of the normal squamous mucosa and beginning of columnar mucosa.. The GOJ and the z-line can lie at the same distance from the incisors or up 2-3cm proximal to the proximal limit of the gastric rugal folds without the presence of a hiatus hernia.

1.1.2 Microscopic Histology of the Normal Oesophagus

The main histological divisions above the striated muscle layers in the oesophagus arethemucosa, submucosa, muscularis propria and the adventitia (Figure 1-1). In the normal human adult, the mucosa consists of an epithelial layer containing non-keratinized stratified squamous epithelium with *keratinocytes*, endocrine cells, Langerhans cells, Merkel cells and T cells with convoluted nuclei. The squamous epithelium is stacked several layers deep. The cells in the basal layer of the epithelium have a large nucleus to cytoplasmic ratio and as the luminal surface approaches, the squamous cells progressively flatten. The basal layer is further subdivided into the papillary layer, which refers to the basal layer that lies atop the basal layers folds, and the interpapillary basal layer which lies between the papillae (Figure 1-1).

Beneath the epithelial layer lies the lamina propria which is a fibrovascular connective tissue compartment which projects up into the epithelium in finger like folds. This lies above the muscularis mucosa which contains longitudinally arranged smooth muscle bundles. Below this the submucosal lies contains a loosely bound network of lymphatics, vessels, lymphoid follicles, Meissner's plexus (sparse ganglia), and submucosal glands. These glands are a continuation of the minor salivary glands of the oropharynx and drain to the luminal surface *via* the submucosal squamous lined ducts (Figure 1-1).

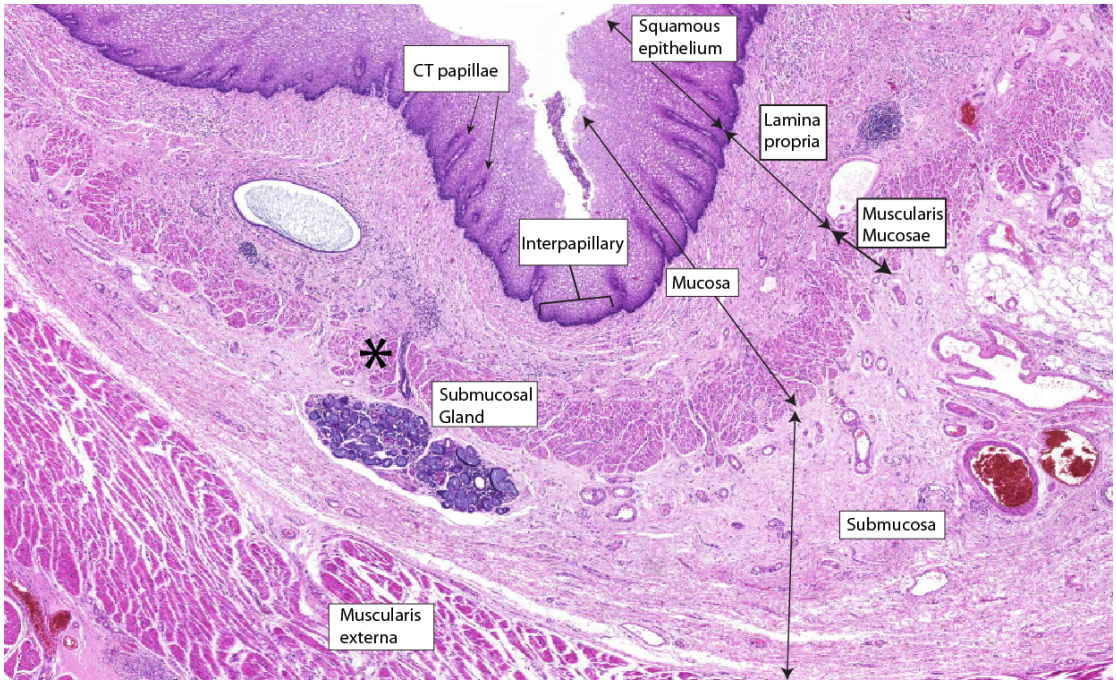

Figure 1-1: Histology of the normal oesophagus.

The normal oesophagus with the lumen above. The squamous lining is the most luminal cell layer and on its basal aspect it is thrown into connective tissue papillae (CT papillae). Beneath this lies the lamina propria which is bounded on its basal aspect by the muscularis mucosa. The squamous epithelium, muscularis mucosae and lamina propria comprise the mucosa. The submucosa lies beneath the mucosa. Circumferential and longitudinal muscle lies beneath the submucosa. Also shown is a deep submucosal gland with a duct leading from it (starred).. These lie in the submucosa and are associated with a squamous lined duct leading to the luminal surface.

1.2 Histology of Barrett's oesophagus pathology.

1.2.1 Microscopic Pathology:

Barrett's oesophagus is defined as the replacement of the normal squamous lined oesophagus with a mucinous columnar lined oesophagus (CLO) typically, but not exclusively interspersed with goblet cells, enterocytes, Paneth cell, endocrine cells (Odze 2008; Odze 2005)andMUC5AC positive foveolar cells (producing Mucin-5AC protein), normally restricted to the epithelium of the stomach.The crypts themselves may show architectural changes such as budding, irregularity, branching, and atrophy (Odze 2006)**.** It is thought that ongoing gastro-oesophageal reflux disease plays an important part and is a common symptom in the development of Barrett's oesophagus (Haggit 1994).

The lamina propria between Barrett's crypts often contains areas of mild inflammation but acute inflammation can also be present in the context of surface ulceration and erosions. The glandular compartment in Barrett's oesophagus (BO) varies according to location with the distal oesophagus containing more gastric-type oxyntic glands than proximal portions (Chandrasoma *et al.* 2001). This is also the case with deep submucosal glands and associated squamous lined ducts.

The importance of mucinous goblet cells (Figure 1-2) in the diagnosis of BO varies between the United Kingdom and the United States: American guidelines state that the presence of goblet cells is necessary for the diagnosis of BO (Spechler *et al.*2011).

This is based on the proposition that goblet cell CLO confers a risk of progression to adenocarcinoma whereas non-goblet cell BO confers a lower risk. However, it is increasingly evident that this is not the caseas up to 70% of metaplastic non-goblet epithelium may show immunopositivity for markers of intestinal differentiation anyway, such as DAS-1, villin and CDX2(Gatenby *et al.* 2008; Kelty 2007). Non-goblet epithelium may demonstrate DNA or chromosomal abnormalities indicating a risk for neoplastic progression (Chaves *et al.*2007; Liu *et al.* 2009; Hahn*et al.* 2009). Other long term studies have also suggested that adenocarcinoma develops with equal risk in goblet and non-goblet cell metaplasia (Gatenby *et al.* 2008; Kelty *et al.* 2007). Furthermore foveolar dysplasia can develop independently of the presence of goblet cells (Chandrasoma *et al.* 2001) As such the definition of BO in this report includes both goblet and non-goblet cell metaplasia (Gatenby *et al.* 2008; Kelty 2007; Takubo *et al.*2009) which is consistent with the current UK guidelines on the diagnosis of BO (Fitzgerald *et al.* 2013).

1.2.2 Macroscopic Pathology of Barrett's Oesophagus:

Endoscopically, BO is recognisable as a salmon pink mucosa distinct from the paler mucosa of the normal squamous surface. Macroscopic recognition is important so that surveillance biopsies can be taken. Scoring systems have been developed to standardise Barrett's length measurements.

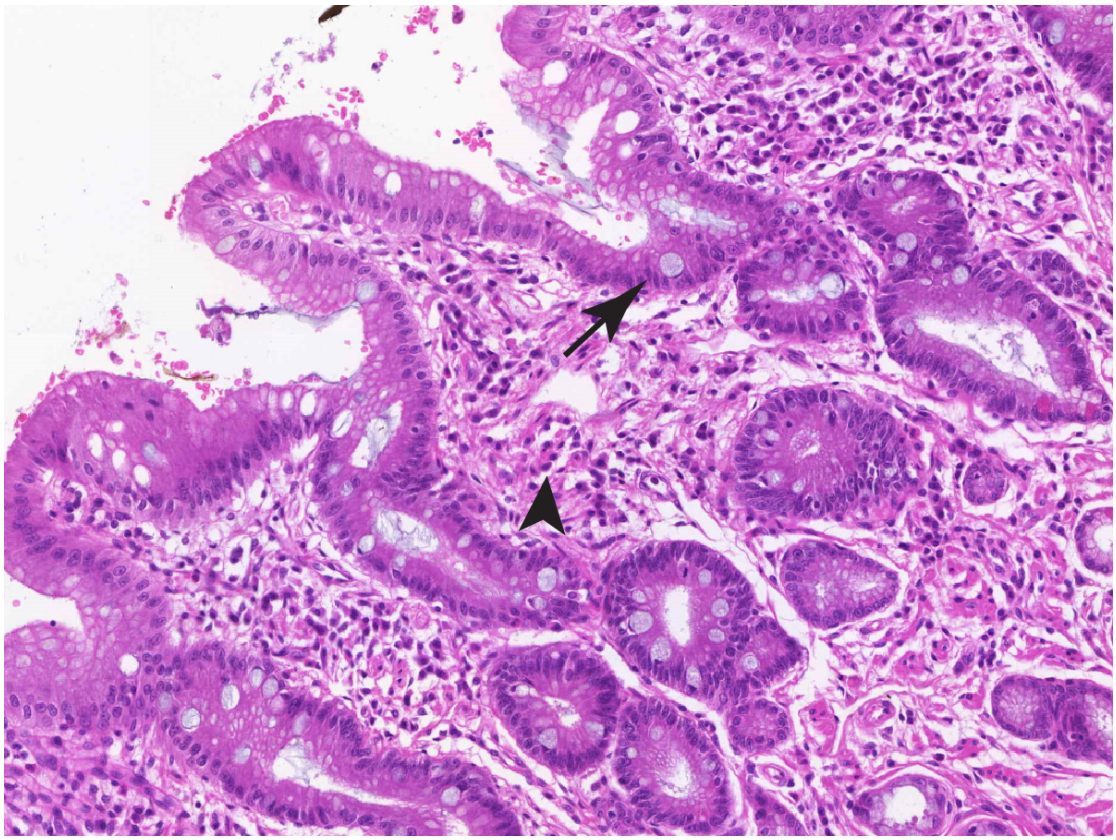

Figure 1-2: Non-dysplastic Barrett's crypts
A Haematoxylin and eosin stain of a non-dysplastic Barrett's characterised by columnar type epithelium. Goblet cells are also present (long arrow) but are not a necessary feature for the diagnosis of Barrett's in the UK. An inflammatory infiltrate in the lamina propria is often associated with this (short arrow)

The most commonly used is the Prague C and M score which requires a measurement of the most proximal extent of the Barrett's segment as well as its most proximal circumferential margin (to distinguish between tongues of Barrett's mucosa) above the GOJ (Sharma *et al.* 2006).

The GOJ is usually located at the same place as the squamo-columnar junction (also called the Z-line). Some individuals have a proximally displaced or irregular Z-line so that the columnar epithelium between the proximal gastric folds and the Z-line is called ultrashort (<1cm) BO. Attempts have been made at sub classifying Barrett's lengths into short (<3cm) and long segment Barrett's (>3cm) but this is of dubious significance. Furthermore, Barrett's epithelium is typically dotted with areas of relatively normal squamous epithelium the source of which appears to locate to deep submucosal glands (discussed later in section 1.4.4).

1.3 Metaplasia dysplasia adenocarcinoma pathway in Barrett's oesophagus

1.3.1 UK clinical surveillance programme for Barrett's oesophagus

Because Barrett's oesophagus can develop into adenocarcinoma in a step-wise fashion, from metaplasia to low grade dysplasia (LGD) through to high grade dysplasia (HGD) and eventually cancer, it is recommended that patients undergo routine endoscopic screening tests. In the UK this is performed every two years in those with metaplasia without dysplasia (also known as non-dysplastic Barrett's oesophagus or NDBO) and more frequently if low or high grade dysplasia is found (Playford 2006). The endoscopist should perform 4 quadrantic biopsies every 2cm from within the affected segment. This is primarily to increase the detection rate of

dysplasia (Reid *et al.* 2000; Reid*et al.* 1988a)which is not always macroscopically visible (Montgomery *et al.*2002; Buttar *et al.*2001)*.*

1.3.2 Histopathology of low and high grade dysplasia.

Dysplasia refers to neoplastic epithelium confined to within the basement membrane and is sub classified into low or high grade dysplasia based on the severity of its cytological features. These features include crowded, elongated cells with hyperchromatic nuclei and an increased nucleus: cytoplasm ratio. HGD may have the additional features of marked loss of cell polarity, atypical mitoses and pleomorphism as well as architectural distortion such as increased crypt complexity and crypt branching and villiform change. Once the dysplastic cells have penetrated through the basement membrane this is known as invasive intramucosal adenocarcinoma, and once the muscularis mucosa has been breached then the lesion is termed an invasive submucosal adenocarcinoma (Montgomery 2001; Reid 1988b).

1.3.3 Risk at each stage of developing cancer.

The overall risk of developing cancer having been diagnosed with NDBO is around 0.33% per year (Desai *et al.* 2012). It also appears that some of the risk is dependent on the stability of the Barrett's NDBO so that the longer a patient's surveillance biopsies have revealed NDBO only, the lower the chance that the patient will ever develop worse pathologies (Gaddam *et al.* 2013).

The risk of progression from low and high grade dysplasia to more severe pathologies is difficult to predict. In one study, 30% of those diagnosed with low grade dysplasia (LGD) on biopsy developed a more severe pathology at a later date (Montgomery 2001). There is also evidence, however, that LGD can regress or remain static for several years (Reid *et al.* 1992; Katz *et al.* 1998; O'Connor *et al.* 1999). Certainly in the short term, LGD seems to remain stable and does not progress to cancer (Miros *et al.* 1991), although the relative instability of LGD versus NDBO is clear when comparing the cumulative risk for HGD or adenocarcinoma development: 85.0% in 109.1 months vs 4.6% in 107.4 months for NDBO (Curvers, ten Kate, Krishnadath, Visser, Elzer, Baak, Bohmer, Mallant-Hent, van Oijen, Naber, Scholten, Busch, Blaauwgeers, Meijer & J. J. G. H. M. Bergman 2010).

Some of the confusion aurrounding the progression rates for patients with low grade dysplasia is derived from the difficulty of the histopathological diagnosis. Because of the subtelties of some of the cellular characteristics of LGD these can be seen in non dysplastic and inflamed tissue. Consequently an approach whereby consensus between histopathologists is reuired for a LGD diagnosis has proven more informative. Using this approach Curvers et al. (Curvers, ten Kate, Krishnadath, Visser, Elzer, Baak, Bohmer, Mallant-Hent, van Oijen, Naber, Scholten, Busch, Blaauwgeers, Meijer & J. J. Bergman 2010) demonstrated that a significant number of biopsies originally graded as LGD could be downgraded to NDBE and that the overall progression rate was 0.44% per year. Of those that had consensus agreement for LGD, the progression rate was 13.4% per year. Confirmed LGD may therefore be of more importance than originally thought.

HGD also has a variable course as regression as well as rapid progression can occur (Weston *et al.* 2000; Rastogi *et al.* 2008; Thomas *et al.* 2005) although once HGD has developed overall it can take several years to progress to adenocarcinoma(Falk et al. 1999; Schnell, S. J. Sontag, et al. 2001; Rastogi et al. 2008) although exact estimates are difficult to determine as HGD and adenocarcinoma can co-exist: 2-33% of oesophagectomy specimens for HGD will also contain adenocarcinoma (Schnell *et al.* 2001; Falk *et al.* 1999; Rastogi *et al.* 2008).

Early adenocarcinoma is still amenable to endoscopic therapy depending on the degree of submucosal invasion. Oesophageal cancer is staged along the tumour node metastasis (TNM) staging protocol which denotes the tumour size (T), the presence of nodes (N) and the presence of metastases (M). Further subclassification involves the degree of submucosal invasion classified as SM1, SM2 or SM3 depending on which third of the submucosa the cancer has invaded (SM1 being the shallowest). Because the risk of lymph node metastases is low for SM1 tumours, whereas the risk increases dramatically with SM2 tumours (Ancona *et al.* 2008; Rice *et al.* 1998), some centres advocate T1SM1 oesophageal cancers as being suitable for endoscopic therapy, with higher stages suitable for surgical resection or palliation only.

1.4 The origins of Barrett's metaplasia

1.4.1 The gastric epithelium as a source of Barrett's oesophagus.

Initial theories on the development of Barrett's oesophagus (BO) concentrated on the possibility of an upward cell migration of the cells from the transitional zone of the GOJ. These cells would colonise the gastric cardia and because of the exposure to refluxate and inflammation, would become columnar epithelial islands which then colonise the distal oesophagus (Hamilton & Yardley 1977).This theory has fallen out of favour following the demonstration that in canine models, in which mucosal strips are taken above a squamous barrier (which itself lies between the gastric transitional zone and the distal oesophagus) , columnar epithelium can still develop despite this intact barrier to migration (Li *et al.* 1994)**.** However, this occurred in only 2 dogs of the 19 studied, and failed to take account of the possibility of buried Barrett's providing continuity with the intact gastro-oesophageal junction (see section 1.8.2.3.3).

A compelling argument for the gastric origins of BO is derived from an understanding of the cells types present. BO contains a mix of goblet cells interspersed with non-goblet columnar cells which resemble gastric foveolar cells. By definition, this is an incomplete type metaplasia, seen in gastric intestinal metaplasia (Correa *et al.* 2010)and is characterised as co-expression of the mucin core MUC5AC, MUC1 and MUC6 which is characteristic of the gastric epithelium, as well as MUC2 and MUC3, characteristic of intestinal differentiation (Glickman *et al.* 2006). This suggests that the specialised epithelium of Barrett's can show evidence of gastric lineage

differentiation as well as intestinal differentiation (Reis *et al.* 1999), although complete intestinalisation (also known as Type I intestinal metaplasia) can also occur (White *et al.* 2008). The similarities between gastric glands Barrett's crypts has support from unpublished observations in our laboratory by demonstration of the similar gene expression distributions between the two tissues. For example, the core mucin protein MUC5AC and the trefoil factor TFF1 are expressed superficially in the pyloric stomach gland, and MUC6 and TFF2 are found at the gland base. This distribution of gene expression is also seen in the Barrett's crypt and is preserved in Barrett's dysplasia.The Wnt target*LGR5*, a *bona fide* stem cell marker in the human colon pathway (Barker & Clevers 2010) is also found in the middle part of the Barrett's crypts on fluorescent *in situ* hybridisation, indicating that the location of the stem cell niche is similar to that of the gastric pyloric gland. Finally, on iododeoxyuridine labelling of cells *in vivo* in human subjects prior to resection, labelled cells can be seen to demonstrate a bidirectional flux whereby the only labelled cells at the end of the experiment were seen in the base and top of the oesophageal crypt, whereas labelled cells were initially seen in the middle of the crypt(Pan *et al.* 2013). This mirrors the bidirectional flux of a normal gastric gland with the gastric stem cell located in the gland neck.

1.4.2 Remnant embryonic cell source from the gastro oesophageal junction as a potential source of Barrett's oesophagus

Putative evidence for gastro-oesophageal cell junctionmigration comes from recent mouse work. Having proposed that p63 null mice develop a columnar lines fore-

stomach, Wang*et al.* isolated the most robustly expressed protein (Car4+, Kr7+) and traced cells in the mouse embryo carrying this protein. In p63 wild type mice, they demonstrated that Car4+, Kr7+ were rendered less proliferative by being undermined and sloughed off when in contact with p63 positive squamous epithelium. Some of the Car4+, Kr7+ cells remained precisely at the squamo-columnar junction (SCJ). In the p63 null mouse, Car4+, Kr7+ cells proliferated throughout the epithelium. In order to test whether Car4+, Kr7+ were the source of the adult Barrett's epithelium, the oesophageal epithelium was damaged by the use of diphtheria toxin and subsequently Kr7+ cells proliferated through the epithelium. Such mouse work has caveats however, namely that the squamo-columnar junction is in the proximal stomach in the mouse, a very different anatomical location to that of the human. Furthermore the metaplasia in p63 null mice may be different to human Barrett's: CDX2, a homeobox gene commonly expressed in BO, was not seen in the mouse model (Wang *et al.* 2011) and the histological phenotype was of a columnar cell monolayer- very different to the glandular structures seen in human Barrett's oesophagus. Another important argument against a SCJ specific origin of Barrett's is the fact 50% of patients who have undergone oesophagectomy which typically involves removal of the squamo-columnar junction, can still develop BO within 2 years after the operation (Wolfsen *et al.* 2004)**.**

1.4.3 Transdifferentiation as a source of Barrett's oesophagus

Transdifferentiation offers a further explanation and refers to the formation of one fully differentiationed state from another(Slack 2007)(Slack 2007)(Slack 2007)(Slack

2007). This occurs during murine embryonic development in which the normal columnar lined oesophagus is converted to a squamous epithelium. Furthermore the cells undergoing this transformation can express markers of squamous and columnar cells(Yu *et al.* 2005). The reverse process may be seen in the human adult in the form of a multi-layered epithelium in which there exists a basal squamous portion and a superficial columnar portion(Glickman *et al.* 2001). However the theory does not account for the fact that ablation of columnar mucosa can result in squamous re-epithelialisation (Shields *et al.* 2001; Barham *et al.* 1997). Furthermore, Barrett's crypt are clonal, a fact that could only be predicted from a true metaplasia resulting from the transcriptional reprogramming of tissue specific stem cells. This has been demonstrated by detecting clonal mutations in the mitochondrial DNA-encoded gene cytochrome c oxidase (CCO) in Barrett's crypt and demonstrating that clonal patches are formed *via* crypt fission (Nicholson *et al.* 2011). This has also been demonstrated in the stomach using the same technology (McDonald *et al.* 2008).

1.4.4 Squamous epithelium as a source of Barrett's oesophagus

An alternative view is that following exposure to environmental stressors such as bile and acid reflux squamous stem cells are induced to form columnar rather than squamous cell epithelium. The location of such a stem cell is still under investigation. A squamous origin, whereby the stem cell population lies within the basal layer of the squamous epithelium derives some support from studies of the squamous interfollicular epidermis which can give rise all skin cell lineages (Alonso & Fuchs 2003).

Human studies assessing proliferation in oesophageal mucosa have demonstrated that proliferation is less frequent in the epithelial basal layer at the top of the papillae and therefore a potential stem cell location (Jankowski *et al.* 1992). Chang et al also found evidence for transdifferentiation by culture of squamous biopsies in retinoic acid (RA). The retinoic acid receptor, in the squamous epithelium is bound by bile acid, a constituent of reflux(Radominska-Pandya & Chen 2002). RA was shown to be upregulated in Barrett's oesophagus and culture of squamous biopsies in RA caused the sloughing off of squamous tissue and the merging of submucosal glands with the luminal surface whilst undergoing some limited columnar differentiation (Chang *et al.* 2007). However the differentiation seen did not emulate the glandular structures characteristic of native Barrett's oesophagus nor did they include the presence of goblet cells so that the transdifferentiation seen may have in fact been a result of the destruction of the squamous epithelium and lamina propria with the subsequent exposure of submucosal glands.

More robust evidence may derive from demonstrating common genomic mutations shared between squamous and columnar lined epithelium. This has been demonstrated with the finding of a shared mitochondrial mutation (Nicholson *et al.* 2011) between the two tissue types adjacent to each other. However the possibility remains that both the squamous and Barrett's epithelium are both derived from the same precursor stem cell which is not necessarily located in the squamous epithelial layer, such as the deep oesophageal submucosal gland or duct (see section1.4.5).

1.4.5 Deep submucosal glands and ducts as a possible source of Barrett's oesophagus

Another potential source of Barrett's stem cells is the duct and gland of the oesophageal submucosal glands which are lined proximally by columnar cells and distally by squamous cells (Leedham*et al.* 2008).This is supported by the finding of a silent *CDKN2A* mutation found in common with a submucosal gland duct and the neighbouring Barrett's epithelium which implies a cell of common origin. Furthermore, using human tissue it has been shown that squamous islands are universally associated with oesophageal gland duct epithelium (Coad *et al.* 2005). An interesting question remains as to whether Barrett's oesophagus contains one stem cell population capable of producing both Barrett's and squamous epithelium or whether these are two separate populations. The demonstration of a mitochondrial mutation shared between squamous epithelium and the adjacent Barrett's suggests that there is only one stem cell population (Nicholson *et al.* 2011) whereas the presence of neo-squamous islands with mutations which are mostly not shared with

the surrounding Barrett's suggests otherwise (Paulson *et al.* 2006) although this paper did show one shared mutation thus continuing the debate as to this source of Barrett's mucosa.

1.5 Genetic and epigenetic aberrations involved Barrett's carcinogenesis

Once metaplasia has developed only a minority of patients will develop dysplastic changes and adenocarcinoma (Desai *et al.* 2012). The progression to adenocarcinoma is marked by several molecular and genetic changes. Although putatively correlations have been attempted between the order of the molecular and genetic changes and the histopathological phenotype, such correlations remain contentious. Although molecular changes exist that are not discussed here, the molecular changes relevant to this report are discussed below. Molecular changes relevant to other areas described in this report are described in the relevant areas.

1.5.1 Tumour Suppressor Genes

Several tumour suppressor genes have been linked to the development of Barrett's adenocarcinoma (Michael *et al.* 1997; Dolan *et al.* 1998), although the most prominent and well validated remain *TP53* and *CDKN2A*.

1.5.1.1 CDKN2A

p16 is an important cell cycle regulatory protein involved in control of the passage from G1 to S phase in response to cellular stress (see section 1.7 for detailed pathways). The locus for the gene responsible for p16, *CDKN2A,* is located at 9p21

and encodes for *CDKN2A* as well as *Alternate Reading Frame* (ARF) each of which has a distinct promoter but which results in alternatively spliced transcripts that share exons 2 and 3. Because the open reading frame for exon 2 is different between the two transcripts, two different proteins are translated (Weber *et al.* 2000; Serrano 1997). p16 inhibits cyclin D kinase 4/6 mediatedhyperphosphorylationof Rb to bind with transcription factor E2F1 leading to G1 cell cycle arrest (Serrano 1997). If the *CDKN2A* locus is lost, then Rb becomes phosphorylated with the subsequent disengagement from E2F which is then available to initiate transcription for entry into the S phase (Rayess *et al.* 2012).

Several mechanisms exist for p16 loss. The p16 promoter can become methylated, the gene can become mutated or can be affected by loss of heterozygosity. The protein expression will be lost when both alleles are affected. Promoter methylation, in which CpG islands in the promoter become methylated,preventing transcription factor binding, has been seen to occur in metaplasia and retained through the metaplasia:dysplasia:carcinoma (MDC) pathway (Hardie *et al.* 2005) in 3-30% of non-dysplastic BO cases (Klump *et al.* 1998; Wong *et al.* 1997). Mutations occur in around 15% of patients with BO with the majority being transitions at CpG sites and insertions/deletion; 60% of these occur at one of three sites: c.172 (R58X), c.238 (R80X) and c.247 (H83Y) (Paulson *et al.* 2008a).

Loss of heterozygosity may also occur in metaplasia (Galipeau *et al.* 1999). This can be a copy neutral event in which two non-functional alleles are inherited from a parental cell, or a copy loss event in which one allele is lost. This is reported to occur in up to 60%-90% of patients with non-dysplastic BO and thus is thought to be the

predominant mechanism for p16 inactivation (Paulson *et al.* 2008a; Barrett *et al.* 1996). The mechanism of allelic damage is less important than the lack of p16 expression. Thus the order and combination of genetic insults to *CDKN2A* does not appear to be important. For example the oesophageal cancer risk when comparing patients with p16 mutation alone versus methylation or loss of heterozygosity (LOH) alone is the same (Paulson *et al.* 2008a).

1.5.1.2 *TP53*

TP53 is a tumour suppressor gene which is considered to be most mutated gene in human cancers (Hollstein *et al.* 1991). It is located on chromosome 17p and encodes the protein p53. The main functions of p53 are to activate the DNA repair mechanisms if damage has occurred, activate p21 mediated cell cycle arrest at the G1/S cell cycle checkpoint, and to initiate apoptosis if the DNA damage cannot be repaired (Zhang *et al.* 2011).

The P53 protein contains 5 major domains. The N-terminal transcription-activation domain (TAD) that activates transcription factors; a proline-rich domain that allows interactions with other proteins; a DNA binding domain (exons 5-8) ; a tetramerization domain crucial for p53 activity *in vivo* and a regulatory C terminus domain. P53 is constantly produced by every cell yet in the absence of DNA damage, murine double minute 2 protein (mdm2) monoubiquitinates p53 and thus it is degraded (Michael & Oren 2003). P53 accumulation occurs when conformational changes initiated by DNA damage or stress, prevent the mdm2-P53 interaction and thus prolong its half-life from minutes to hours.

TP53 mutations are relatively uncommon in non-dysplastic Barrett's mucosa (Novotna *et al.* 2006), although possibly more common if the non-dysplastic area is associated with a cancer elsewhere in the oesophagus (Schneider *et al.* 1996) whereas in adenocarcinoma they can be found in up to half of cases (Catalogue of somatic mutations (http://cancer.sanger.ac.uk/cosmic/gene/analysis?ln=TP53#histo). This indicates that *TP53* mutations may occur later in Barrett's progression; LOH of *TP53* can occupy large areas of the Barrett's oesophageal mucosa *via* clonal expansion (Galipeau *et al.* 1999).

1.5.1.3 Epigenetic changes

Methylation of gene promoters is also thought to be important in the progression to Barrett's adenocarcinoma. Initial studies concentrated on tumour suppressor gene hypermethylation as discussed with *CDKN2A* (see section 1.5.1.1). Frequent hypermethylation in adenocarcinoma samples has also been demonstrated for a number of other genes on targeted analysis such as*Adenomatous polyposis coli* (*APC)*, *Estrogen receptor 1* (*ESR1)* and *cadherin 1* (*CDH1)*(Kawakami *et al.* 2000)(Eads *et al.* 2000) and others although the exact role of methylation in the progression to adenocarcinoma has not been fully elucidated. To confuse matters, genome wide methylation studies have suggested global hypomethylation may also be an important mechanism during carcinogenesis and that progressors were more likely to demonstrate global hypomethylation during progression to adenocarcinoma(Wu *et al.* 2013; Agarwal *et al.* 2012). Thus selective hypermethylation of targeted genes on a background of global hypomethylation may be a characteristic of Barrett's progression.

1.5.1.4 Other genes and aneuploidy

Systematic unbiased sampling of genomic mutations in oesophageal adenocarcinoma have very recently come to publication. This has become possible since the advent of newer high throughput technologies such as next generation sequencing. Such studies have not only confirmed that *TP53* and *CDKN2A* are frequently mutated in adenocarcinomas but also that chromatin remodelling genes such *ARID1A* and *SMARCA4* (members of the Switch/ sucrose nonfermentable-complex) are mutated in at least a quarter of oesophageal adenocarcinomas

(Streppel *et al.* 2013; Dulak *et al.* 2013). This provides further evidence for the role of epigenetic modifications in the progression to Barrett's adenocarcinoma.

Several other novel mutations have also been discovered using these newer technologies including *ELMO1* and *DOCK2*, constituents of the RAC1 GTPase pathway (Dulak *et al.* 2013) which has been implicated in cancer invasion, decreased apoptosis and increased cell survival (Wertheimer *et al.* 2012). SMAD4, a gene involved in TGFβ signalling pathway has also been confirmed as being mutated in a significant number of adenocarcinoma samples (Dulak *et al.* 2013), although it is also likely to lose further expression through promoter methylation (Onwuegbusi *et al.* 2006).

Weaver et al. have also recently published a comprehensive whole genome analysis with amplicon resequencing of 112 oesophageal adenocarcinomas (Weaver et al. 2014). They demonstrated that the majority of mutations present in non-dysplastic mucosa were also present in the non-dysplastic Barrett's, and that *TP53* and *SMAD4* mutations occurred in a stage specific manner. In particular they highlighted that non-dysplastic Barrett's mucosa was highly mutated perhaps underlining the idea that idea that individual mutations are unlikely to be as important as the context they exist in.

Aneuploidy refers to the presence of cells with a chromosome number other than 2N (diploid) or 4N (tetraploidy). Aneuploidy does not correlate single gene mutations but rather with overall genomic instability. Aneuploidy exists in over 90%ˆof HGD and adenocarcinoma and the presence of an aneuploidy population is correlated with Barrett's progression to adenocarcinoma (Reid. *et al.* 2000). It is thought to

occur late in this progression (Barrett *et al.* 1999). Although it has been suggested that this could be used particularly in low grade dysplasia as a predictor of progression to adenocarcinoma (Teodori *et al.* 1998) some authors have suggested that correlation with histology is not robust (Reid *et al.* 2000).

1.6 Field cancerization and Barrett's metaplasia

1.6.1 Introduction:

The concept of a metaplasia:carcinoma sequence (MCS) pathway is consistent with the idea that somatic mutations, as well as other genetic aberrations found within cancers, can be found in morphologically normal tissue before a cancer develops**.** This concept was first proposed in the context of the head and neck squamous cancers (HNSCC) (Slaughter *et al.* 1953). Initial observations had demonstrated that HNSCC tumours frequently arise multifocally and that there was a significant risk of the development of metachronous tumour development. Slaughter and colleagues proposed the explanation for this was "preconditioning of an area of epithelium to cancer growth by a carcinogenic agent" (Slaughter *et al.* 1953). Subsequent work has demonstrated that the area or field of epithelium apparently predisposed to cancer development can often share a common genetic aberration, such as a somatic point mutation, suggesting that the field is clonal in origin(Braakhuis *et al.* 2005). Thus field cancerization studies now focus on understanding how the mutant clones that ultimately lead to a "field-defect" are established and spread.

There is increasing evidence that field cancerisation occurs in a variety of tissues. Sampling of the tracheobronchial tree of one individual with a long history of

smoking without lung cancer, revealed the same mutation in *TP53* in seven out of 10 sites studied (Franklin *et al.* 1997). That such field cancerization may lead to cancer has been detected using LOH at chromosome 12p in normal bronchial epithelium of long-term smokers which was also observed in non-small cell lung cancers in the same patients (Grepmeier *et al.* 2005). In the pancreas, analysis of microdissected, morphologically normal, peritumoral tissue (intraductal papillary-mucinous tumours) has demonstrated identical mutations as were present in the tumour (Kitago *et al.* 2004). Similar findings have been found in the bladder (Simon *et al.* 2001), prostate (Hanson *et al.* 2006), breast (Deng *et al.* 1996) and colon (Galandiuk *et al.* 2012).

1.6.2 How Does An Epithelial Field Become Cancerized?

The process that leads to a cancerized epithelial field is mechanistically poorly understood. Assessment of such a mechanism has relied on studies demonstrating the growth patterns of clonal populations of cells, that is, cells which share a common ancestry. Such clonality studies rely on the demonstration, for example of a shared somatic mutation, common methylation patterns or shared LOH patterns: data that have often been used in understanding cellular dynamics in the colon. The colonic epithelium is pitted with invaginations called crypts; the putative stem cell- the parent cell of the epithelium within each crypt- is located at the base of the crypt (Snippert *et al.* 2010; Barker & Hans Clevers 2010). The mechanism by which a mutated stem cell may occupy a colonic crypt occurs by a process of niche succession, whereby one stem cell comes to dominate the niche in the crypt base which is the site of the putative stem cell, and monoclonal conversion, whereby the crypt epithelium is composed of the progeny of the dominant stem cell. This results

in a fully clonal crypt (Barker *et al.* 2007; Ponder *et al.* 1985). The mechanism by which this mutated crypt then propagates the mutation is likely to occur through a process of crypt fission (Greaves *et al.* 2006).

During post-natal development of the gastrointestinal tract there is a need to populate the gut with crypts. This occurs by crypts initially bifurcating at the base and then separating longitudinally to produce two daughter crypts. During post-natal development this process, known as crypt fission, occurs very frequently (Maskens & Dujardin-Lotis 1981)**.** The process is not however limited to development and is up-regulated during healing of ulcerative colitis lesions (Cheng *et al.* 1986) as well as during regeneration after exposure to ionizing radiation (Cairnie & Millen 1975) or chemotherapy (Wright & Al-Nafussi 1982)and after inflammation (Cheng *et al.* 1986)**..**It is also likely to be a mechanism to explain field cancerization; analysis of a dysplastic crypt caught in fission demonstrated that both arms contained *TP53* allele gains with a single chromosome 17 centromere, and that these features were not present in the surrounding crypts (Chen *et al.* 2005).

Crypt fission is thus considered to be the canonical method of clone spread in the colon. It can also be seen in the stomach (McDonald *et al.* 2008) and small intestine (Gutiérrez-González *et al.* 2009) . The progression to gastric adenocarcinoma is marked initially by the development of gastritis with the subsequent epithelial conversion to intestinal metaplasia (Correa & Shiao 1994)**.** The field containing intestinal metaplasia can develop dysplastic changes which can lead to invasive disease. Using laser capture microdissection and assessment of the presence of somatic mutations on a gland by gland basis, it has been shown that a large

dysplastic field can arise from one gland containing intestinal metaplasia, demonstrating the existence of field cancerization in the stomach. Furthermore using non-functional mitochondrial mutations, it can be shown that patches of gastric glands share a common mitochondrial mutation, whereas immediately surrounding the patch glands are wild type (Gutiérrez-González *et al.* 2011). The replication of a gland such that it is monoclonal and identical to its neighbour can only practically be explained by a fission process.

By extrapolation therefore, can crypt fission be used to explain the spread of field cancerization in the columnar oesophagus? The mechanism of spread of the field has proved more difficult to elucidate than elsewhere in the gastrointestinal tract as it can look histologically more disorganised and increasingly so when field becomes dysplastic. The demonstration that patches of crypts are clonal for mutations is a useful surrogate for the process of crypt fission having taken place. As in the stomach, a common mitochondrial mutation has been demonstrated in localised patches of oesophageal crypts and it seems likely that crypt fission plays an important role in field cancerization in the oesophagus (Nicholson *et al.* 2011) although confirmation is needed.

The mechanism that regulates fission is not understood. It has been suggested from mathematical models, that the increase in stem cell numbers could cause the epithelial sheet to buckle and therefore initiate fission (Edwards & Chapman 2007). Furthermore, because crypt fission is increased in the adenomas of patients with familial adenomatous polyposis- an inherited colorectal condition predisposing patients to the development of numerous colonic polyps - the gene *APC*

(adenomatous polyposis coli) which is mutated in this condition, has also been implicated in regulating fission (Wasan *et al.*. 1998).Whether this is a direct effect on the control of the fission rate, or as a result of alterations to the stem cell population remains unclear.

Regardless, it seems likely that fission could account for the ability of clones to travel large distances through the gastrointestinal (GI) tract. Large fields of monoclonal cancerization have been demonstrated in the oesophagus, stomach and gastrointestinal tract: the same p16-mutation has been demonstrated throughout a 16cm segment of Barrett's oesophagus (Galipeau *et al.* 1999). Recently a Crohn's patient has been described with a common mutation demonstrated in the rectum, ascending colon and terminal ileum (Galandiuk *et al.* 2012). Dysplastic areas covering a large proportion of the stomach surface have been shown to have the same somatic mutation(Gutiérrez-González *et al.* 2011)**.**Given the presence of inflammation in Barrett's and Crohn's, it is therefore possible that the increased crypt fission rate that is known to occur in inflammation, is responsible for the distances travelled by the clones.Field cancerization in Barrett's oesophagus had been suggested to be due to the growth of a single clone throughout the entire Barrett's segment (Wong *et al.* 2001)based on clonal analysis of whole biopsies. Although it is likely that patches of BO are monoclonal and that these patches are a result of ongoing crypt fission, laser microdissection and genetic analysis of individual Barrett's crypts has demonstrated that the field of cells predisposed to cancer may contain several genetically distinct clones; prior studies showing

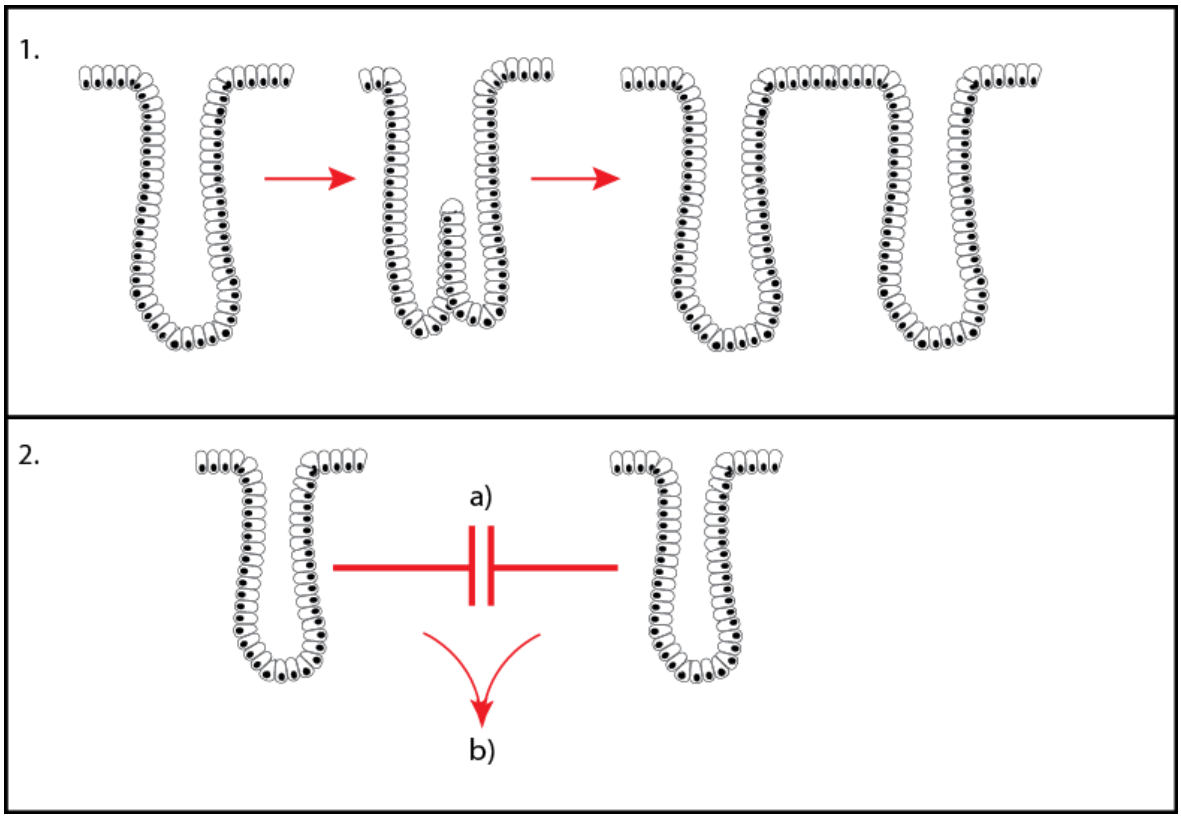

Figure 1-3:Clonal expansion in Barrett's
Crypts are seen in cross section on the diagram. 1)Crypt fission is the canonical mechanism by which field cancerization occurs in the gastrointestinal tract. The crypt division starts at the base and progresses longitudinally. 2) The consequences of field cancerisation may be that spatially separate clonal populations interact via a) Cellular competition b) Cellular co-operation or via interaction with the stroma.

monoclonality of lesions were possibly confounded by the sequencing of whole biopsies, rather than individual crypts, which may mask mutations present at low frequency (Leedham*et al.* 2008). Genetic diversity within a Barrett's segment is predictive for the risk of progression to adenocarcinoma (Maley *et al.* 2006). These observations raise the possibility of clonal interaction as a driving force for carcinogenesis. Such clonal interaction could take many forms, such as clonal co-operation, clonal competition and interaction of clonal populations with the stroma.

1.6.2.1 Clonal interactions

1.6.2.1.1 Clonal competition

An interesting possibility involves clonal competition. The concept of competition in biological systems has been well studied in the field of ecology. It is most simply defined as the interaction of two species (interspecific) or two members of one species (intraspecific) which leads to the removal or depletion of another species' resource. A resource is defined as an element that is consumed by an organism, can be depleted, is used for maintenance, growth, or reproduction and reduces population growth when its availability is limited (Keddy 2001).

The elements of such a definition are therefore:

a) The competitors should (usually) neighbour each other.

b) A limiting resource that is competed over.

c) The competitors should have a detectable effect on each other so that the removal of one competitor results in removal of that competitive effect for the remaining element.

The status of 'competitor' is context dependent so that a species does not demonstrate competitive behaviour when not in proximity with a competing species.Competitive modes of cellular interaction have been described predominantly in *Drosophila melanogaster*. Having created a Drosophila strain which was chimeric for cells with genes expressing a ribosomal protein known as Minutes (M), immunohistochemistry and *in situ* immunofluorescence has been used to demonstrate that wild-type (Wt) cells could repopulate the chimeric wing epithelium and that the cells at the border between M/Wt and Wt/Wt demonstrated apoptosis (Morata & Ripoll 1975). Further work using the same chimeric-fly model has established further characteristics of cellular competition in Drosophila. Competition appears to occur between cells of different clonal origin and this competition is proximity dependent. The induction of apoptosis is considered the primary mechanism of competition; cells not located at a clone border are unlikely to apoptose. Further, the death of a cell in one clone cell stimulates proliferation of cells in the competing clone. Finally, competition does not alter wing homeostasis; in the case of the imaginal disc, the disc remains normal in structure and function irrespective of the competitive processes within it (Simpson & Morata 1981).

The central role for apoptosis as the driver of the rival clone's growth has been further demonstrated by the use of baculovirus p35 protein to block the apoptotic machinery which has the result of reducing the ability of winner cells to

proliferate(Moreno *et al.*2002)**.** Interestingly, transgenic tumour cells induced in flies have also been shown to be the "loser" in cell competition experiments. Apical-basal polarity genes discs large (dlg), scribble (scrib) or lethal-giant larvae (lgl) help to orientate cells within the Drosophila imaginal discs (the wing precursor). Constitutive mutations of any of these genes cause fatal neoplastic growth in the developing embryo. However constitutional mosaics with homozygous mutations do not form tumours and homozygous mutated areas are engulfed by wild type epithelium (Rhiner *et al.* 2010).

Based on the Drosophila experiments it has been proposed that competition may play a part in field cancerization(Rhiner & Moreno 2009). Field changes have been demonstrated in mammalian systems. Chimeric rat livers can be created by transplantation of foetal liver progenitor cells into hosts. Oertel *et al.* have transfected progenitor hepatocytes and hepatoblasts with a lentivirus containing a reporter gene- green fluorescent protein (GFP) (Oertel *et al.* 2003). When regenerative stimulation occurs by performing a partial hepatectomy in the recipient rat, and subsequent stimulation of the reported gene, the younger donor cells can be seen to respond vigorously and eliminate the host cells by apoptosis until an entirely donor derived liver is generated (Oertel *et al.* 2003).

However, the apparently central role of apoptosis in Drosophila models of cellular competition described above has not been reflected in luminal gastrointestinal neoplasia. Therein, even in high-grade dysplasia, markers for apoptosis are not common (Katada *et al.* 1997; Wetscher *et al.* 1998), although it should be noted that most studies have not been designed to examine putative-competition at clone

borders *per se*. Thelack of apoptosis in luminal dysplasia does not necessarily mean that competition is not occurring in these tissues; apoptosis may also not be the only expense that a 'loser' cell population pays. Other potential cell behaviours such as cell cycle arrest and senescence, or even the induction of a slower proliferation rate, could conceivably be induced by 'winner' cells in the neighbouring loser populations- this has yet to be assessed.

1.6.2.1.2 Clonal co-operation

Clonal co-operation in which two clonal populations are mutually protumorigenic, has also been documented. Using mitotic recombination *Drosophila melanogaster* can be engineered so some of the epithelial cells in the eye antennal imaginal discs lack the Ras oncogenic protein (Ras^{V12}), and others lack scribbled ($scrib^{-}$). The combination of cells produces tumours far larger than lack of either gene alone, through upregulation of JAK/STAT-activating cytokines (Wu *et al.* 2010). This has also been demonstrated using human cell lines recapitulating the brain tumour glioblastoma. The tumour often contains a mutated epidermal growth factor receptor (EGFR) which is present with far less abundance than the wild type EGFR but nevertheless maintains the tumour growth and heterogeneity through the paracrine effect of IL-6 and leukaemia inhibitory factor on the EGFR wild type cells (Inda *et al.* 2010).

1.6.2.1.3 Clonal demographics

A further important omission in the description of clonal interactions is an intimate description of the demographics of clonal populations. Clonal populations must neighbour each other but this does not necessarily imply a straight border between the populations. Certainly clonal populations in drosophila models adhere to definite borders when apposed resulting in apoptosis of cells along the border of the less robust population (Morata & Ripoll 1975). Such straight borders have also been demonstrated in the colons of human females heterozygous for X-linked polymorphisms such as can be found in the gene glucose-6 pyruvate dehydrogenase. Because of random X-linked inactivation during embryogenesis, these females are functionally mosaic at the mRNA level so that clonal populations can be visualised with immunohistochemical stains (Novelli *et al.* 2003). Although not specifically assessed in Barrett's, the clonal populations do not seem to share such a neat border with the populations being rather more intermixed (Leedham *et al.* 2008) Such demographic descriptions are important not only in terms of describing how clonal populations may interact but also as a description of the effect of clonal interactions. It has been proposed that clonal populations with a similar fitness can slow each other's evolution, as characterised by the acquisition of new mutations, when these populations collide (E. Martens & Hallatschek 2011).

1.6.2.1.4 Genetic heterogeneity

Genetic heterogeneity is a prerequisite for clonal interactions to occur. Such heterogeneity refers to the presence of several clonal populations in a tumour where

clonality can be defined as a genetically identical subpopulation of cells descended from a most recent common ancestor cell so that thesubpopulation inherits the genetic aberrations of its parent (Kostadinov *et al.* 2013). The presence at different stages of carcinogenesis, as well as the spatial and temporal manifestations of heterogeneity within a tumour, are beginning to be clarified. As such most GI premalignant lesions are thought to be monoclonal although exceptions do exist such as familial adenomatous polyposis (H. Clevers 2011)as well as Barrett's oesophagus (Leedham*et al.* 2008).

The spatial characteristics of heterogeneity are also important to define in order to determine the nature of clonal interactions. Clonal populations can exist in geographically disparate areas (Gerlinger *et al.* 2012) as well as being well mixed (Inda *et al.* 2010). Crypt by crypt analysis of oesophagectomy specimens from patients with Barrett's related adenocarcinomas indicates that some intermixing may exist in Barrett's related dysplasia so that any clonal interaction may be with a nearest neighbour rather than a population effect (Leedham*et al.* 2008).

Heterogeneity is further complicated by a lack of temporal stasis particularly after therapy is applied to a tumour. Such temporal heterogeneity whereby clones may become more or less dominant over time has been demonstrated haematological malignancies after chemotherapy (Landau *et al.* 2013) when a previously subdominant clone becomes dominant after chemotherapy has reduced the burden of the originally dominant clone. Changes in clonal dominance over time have also been seen after non-steroidal anti-inflammatory medication in Barrett's oesophagus (Kostadinov *et al.* 2013). Given this temporal heterogeneity it would also be

intriguing to determine how clonal populations vary with clinical response to other therapies for Barrett's such as endoscopic ablation.

1.6.3 Selective advantages of clonal populations

Although I have discussed several possible mechanisms for the growth of a mutant clone, the consistent proliferation of any particular clone requires it to have a selective advantage compared to other clonal populations. Several different cellular phenotypes may confer such a selective advantage. Mutations of *CDKN2A* can prevent production of functional p16 protein and therefore encourage cells to escape or prevent senescence (Hardie *et al.* 2005). *CDNK2A* LOH, whereby one allele of the gene is damaged, has been recognised as an event that can occur at the metaplasia stage in progression to oesophageal cancer in the context of Barrett's oesophagus, as has methylation of its promoter region and point mutations(Wong, Paulson, L J Prevo, et al. 2001)The selective advantage conferred by the mutation in this case could therefore be an escape from oncogene-induced or replicative senescence.Although generally occurring later in the metaplasia-dysplasia-carcinoma progression, the gene *TP53* that produces the tumour suppressor protein p53 can also be mutated. When functioning normally, one of the roles of the p53 is to control apoptosis in response to cellular damage from a number of sources. Thus the selective advantage may be as a result of apoptosis resistance.

1.6.4 The clinical importance of field cancerization

Field cancerization can be demonstrated in many different tissues. The gastrointestinal tract is of particular interest because of the burden of disease in this organ in Western populations (Siegel *et al.* 2012). Gastroenterologists have long been aware of the cancerized field within the oesophagus, stomach and colon. Barrett's oesophagus in particular has a small risk of progression to adenocarcinoma but enough to warrant many countries to engage in endoscopic surveillance on a routine basis. These surveillance programmes have also been extended to colonoscopic surveillance particularly for high risk conditions such as inflammatory bowel disease (Cairns *et al.* 2010). Such programmes are often unpleasant for patients, not without inherent risk and are expensive. The discoveries that field cancerization will provide may lead to biomarkers that will be able to stratify patients by cancer development risk, rather than simply being biomarkers for the presence of the disease. By demonstrating that certain molecular changes within precancerous fields increase the risk of malignancy, patients with those particular changes could be streamlined into a regular surveillance programme. Similarly, those without the high-risk molecular changes may not need to be surveyed. Although such molecular biomarkers have not come to full fruition in gastroenterology there are several avenues that are promising. As an example, LOH of *TP53* identifies patients with Barrett's oesophagus who are likely to progress from non-dysplastic or low grade dysplasia to high grade dysplasia (Reid *et al.* 2001). Patients with aneuploidy and tetraploidy, which usually occurs after *TP53* inactivation and is detectable by flow sorting of biopsies from Barrett's oesophagus, are also more

likely to progress to adenocarcinoma (Rabinovitch *et al.* 2001).Thus molecular abnormalities within a cancerized field could conceivably be used to stratify patients according to risk.

A further important implication of field cancerization is considering how much to resect when surgically removing a tumour. Currently assessment of surgical margins relies on demonstrating the absence of cancer infiltration at resection margins. As an example, a clear margin at oesophagectomy for Barrett's related adenocarcinoma relates to an improved prognosis (Dexter et al 2001). Complementing this with molecular studies to demonstrate that resection margins do not share the genetic abnormalities of the field from which the resected cancer arose may provide further prognostic information. For example, 53% of patients with a *KRAS* codon 12 mutation within normal resection margins following resection of pancreatic adenocarincoma were subsequently found to have an unfavourable prognosis when compared to normal molecular margins (Kim *et al.* 2006). Furthermore extension of routine resection margins for cancers that may exist in large areas of field cancerization, may improve cure rates. Field cancerization of Barrett's oesophagus may extend a considerable distance (Galipeau *et al.* 1999). Similar reports have been noted in a Crohn's colitis patient in whom the mutation responsible for a locally resected rectal tumour was found in the ascending colon and terminal ileum and gave rise to further adenocarcinomas (Galandiuk *et al.* 2012). It is conceivable then, that localised resection could prove inadequate to prevent tumour recurrence.

Quite apart from Barrett's oesophagus, studies in field cancerization may also lead to an understanding of non-pathogenic tissue repopulation, and therefore may answer

some fundamental questions regarding tissue development and cell population homeostasis. Tracing the distribution of a clonal cell population by the use of somatic or mitochondrial mutations has already been used to determine how cells can clonally repopulate a colonic crypt. The principles of field cancerization can also be applied to transplant medicine to determine how repopulation of a tissue can occur with the implantation of a healthy cell population. Thus cell transplantation rather than whole organ transplantation would benefit from understanding how a clonal population comes to dominate a field although in this context it would be to create a healthier organ rather than one at risk of developing cancer. This development and maintenance of healthy tissue populations from implanted cells has started to be investigated in gastroenterology (Oertel *et al.* 2003; Uccelli *et al.* 2008).

1.7 Senescence in Barrett's oesophagus

1.7.1 Overview of cellular senescence

Borrowing from ecological definitions (see section 1.6.4), interacting clonal populations should have a detectable effect on one another. Mechanisms of clonal interactions have not been described in human cells either *in vivo* or *in vitro* although cells from the same population can have a range of effects on each other's behaviour.

One such interaction may be cellular senescence. This refers to irreversible cell growth arrest which can occur with the appropriate oncogenic stress (Rodier &Campisi 2011). It was originally described in the context of a process that limited

the number of times a cell can divide known as Hayflick's limit (Hayflick 1965). Although we now know this to be only one aspect of cellular senescence, escape from senescence is now deemed to be one of the hallmarks of cancer (Hanahan & Weinberg 2011). It is becoming increasingly apparent that senescent cells can affect neighbouring cells either of the same or different type although the nature of this influence is still a matter of debate. Senescence is a cellular response to a range of different insults and is abundant in Barrett's oesophagus (Going *et al.* 2002) . It therefore represents a potential model to demonstrate a mechanism of intercellular interactions.

1.7.2 The induction of senescence.

Understanding the causes of senescence also allows us to sub-classify it. The original description is known as replicative senescence and is a telomere dependent process (Hayflick 1965). DNA damage, especially that which causes double strand breaks, can also cause a cell to undergo senescence(Parrinello *et al.* 2003). Senescence in this context is strongly p53 dependent accompanied by p21 expression (DiLeonardo *et al.* 1994), and can also induce p16 as a second pathway to maintain growth arrest (Krishnamurthy *et al.* 2004; Jacobs & de Lange 2004). DNA damage can be caused by a variety of different insults such as ionizing radiation (Mirzayans*et al.* 2005; Tsai*et al.* 2009). and chemotherapeutic insults (Herbig*et al.* 2004).

Oncogenes can also be potent inducers of senescence. The oncogenic form of Ras and members of its pathway are well known to induce senescence in fibroblasts (Dimri *et al.* 2000; Lin *et al.*1998; Michaloglou *et al.*2005).Senescence in this context

may act to counteract excessive mitogenic stimulation. The pathways involved in oncogene induced senescence may be similar to telomere induced senescence in that oncogene induced senescence (OIS) can induce a DNA damage response and can also induce p16 and senescence associated heterochromatin foci (SAHF) formation (Narita *et al.* 2003; Ohtani 2001). Although oncogene induced senescence does not occur in all cells (Benanti & Galloway 2004), it is still relevant to the development of cancer in mammalian systems. Activated oncogenes producing strong mitogenic signalling in mice produce lesions consisting of senescent cells, andbenign naevi in human skin contain cells that express oncogenic BRAF and are senescent (Colladoet *al.* 2005; Michaloglou *et al.* 2005).

Finally, senescence can be induced by a range of other stimuli loosely collected under the title of stress. For example, chronic interferon stimulation induces a p53 dependent DDR and subsequent senescence response (Campisi& d' Adda di Fagagna 2007). Cell culture stress (culture shock) such as inadequate or hyperphysiological growth conditions can also induce a p16 dependent, telomere independent senescence response, as can oxidative stress (Ramirez*et al.* 2001), which may or may not be p16 dependent (Itahana *et al.*2003).

1.7.3 Senescence pathways

Regardless of the many and disparate causes of cellular senescence, its initiation seems to depend on major tumour suppressor pathways controlled by p16/Rb (phosphorylated retinoblastoma protein), as well as by p53 (see Figure 1-4). p16 is a cyclin dependent kinase inhibitor and is able to bind both CDK4 and 6 (Rocco

&Sidransky 2001) (see section 1.5.1.1). p53 is also a central senescence initiating pathway involving p21 is also a cyclin dependent kinase inhibitor, which prevents cell-cycle progression by inhibiting the activity of cyclin E-associated CDK2. Its transcription from *CDKN1A* is under the direct control of p53. The relative contributions of the p16-Rb and p53 pathway to senescence are unclear. Phenotypic changes exist, however, that are common to both:

a) Irreversible growth arrest. Occasionally, p53 suppression can reverse senescence in p16 inactivated cells although this has never been seen *in vivo* (Beausejour *et al.* 2003).

b) An increase in cell size (Hayflick 1965).

c) They express senescence associated β-galactosidase which identifies lysosomal β-D-galactosidase, an enzyme which is expressed as part of the increased lysosomal compartment that characterises senescent cells (Dimri *et al.* 1995).

d) Unless unable to, most senescent cells express p16 which itself can activate the formation of senescence associated heterochromatin foci, nuclear DNA domains enriched for histone modifications (Narita *et al.* 2003).

e)In the context of persistent DNA damage response signalling, senescent cells secrete a range of proteases, cytokines and other factors which is termed the senescent associated secretory phenotype This has powerful autocrine and paracrine effects which can be pro and anti-tumorigenic (Acosta *et al.* 2008; Kuilman *et al.* 2008) (see section 1.7.4).

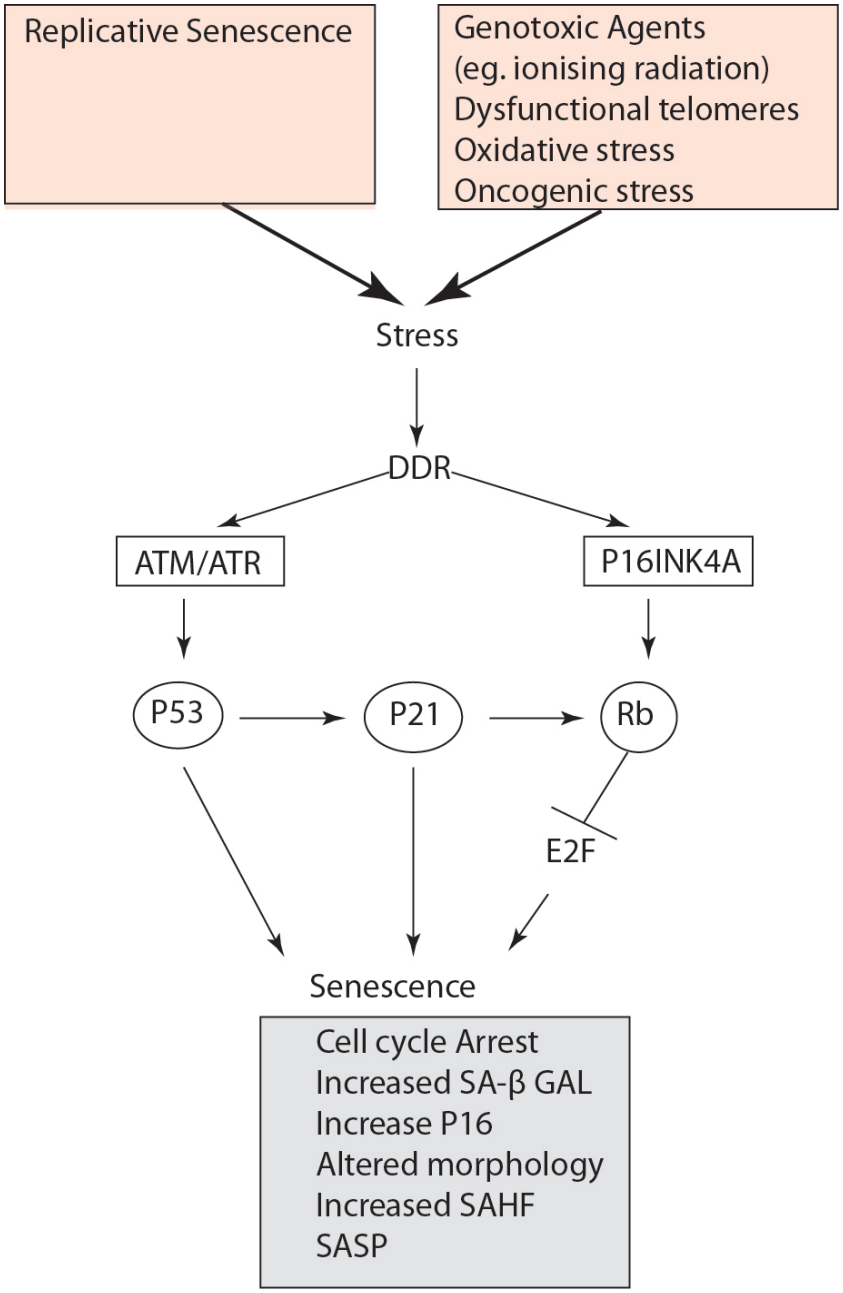

Figure 1-4: Overview of major senescence pathways.

The two most important are the p53-p21 pathway and the p16-Rb pathway. Both pathways are activated in response to a range of cellular insults which result in upregulation of the DNA damage response pathway. The p53-p21 pathway is activated in response to the presence of human protein kinases ATM (ataxia-telangiectasia, mutated)/ATR (ATM and Rad3-related). SA-β Gal= Senescence associated β galactosidase; SAHF= senescence associated heterochromatin foci; SASP= senescence associated secretory profile.

1.7.4 The pathology of senescence- the senescence associated secretory profile

Senescence has been well studied in the context of cancer. Mutations in *CDKN2A*, *Rb* or *TP53* pathways exist in most cancers, and markers of senescence are reduced in cancers, whereas their premalignant counterparts such as malignant human naevi and colorectal adenomas show abundant senescence (Bartkova *et al.* 2005; Michaloglou *et al.* 2005).

However senescence may be more complex than simply a mechanism to cause growth arrest in damaged cells. Cells that have undergone a growth arrest continue to be metabolically active. Large scale mRNA arrays have demonstrated that there is a plethora or expressed factors; this is now termed the senescence associated secretory profile (SASP) and has been demonstrated as a relatively well conserved expression profile in a number of human cell types including liver stellate cells(Schnabl *et al.* 2003)endothelial cells (Shelton *et al.* 1999), and epithelial cells of the retinal pigment, mammary gland, colon, lung, pancreas, and prostate (Collado *et al.* 2005; Coppe *et al.* 2008; Shelton *et al.* 1999; Schwarze *et al.* 2002). The SASP consists of a several families of proteins which can be broadly divided into two major categories: soluble signalling factors (interleukins, chemokines and growth factors), secreted proteases, and secreted insoluble proteins/extracellular matrix (ECM) components such as matrix metalloprotein members (MMP) (Liu & Hornsby 2007; Millis *et al.* 1992) and serine proteases (Comi *et al.* 1995). Of the former category, IL-6 and IL-8 are the most prominent. The expression of these cytokines has been associated with DNA damage and oncogenic stress–induced senescence of mouse and human keratinocytes, melanocytes, monocytes, fibroblasts, and epithelial

cells(Coppe *et al.* 2008; Kuilman *et al.* 2008; Lu *et al.* 2006). They are also under direct regulation by the DDR and are upregulated in response to ATM (Rodier *et al.* 2009). IL-1 is similarly upregulated in senescent cells (Bode-Boger *et al.* 2005; P *et al.* 2003; McLachlan *et al.* 1995). IL-8 secretion is accompanied by an upregulation of IL-8 receptor expression possibly as a mechanism of self-regulation of senescence (Acosta *et al.* 2008). Within this category, other secreted factors such as the insulin growth factor family and colony stimulating factors(Wang *et al.* 1996; Coppe *et al.* 2008)are also secreted.

The effect of SASP is manifold. One of the most prominent effects is the proliferation of epithelial cells. Proliferation of premalignant and malignant breast epithelial cells can be stimulated by senescent fibroblasts (Coppe *et al.* 2008; Krtolica *et al.* 2001) as can prostate epithelium (Bavik *et al.* 2006). Increased cell migration, invasion, and promotion of leucocyte recruitment (Xue *et al.* 2007; Coppe *et al.* 2008) are also documented effects of the SASP.

The SASP may be particularly relevant in the context of ionizing radiation. It is well documented that cells in contact with cells that have undergone ionizing radiation induced senescence demonstrate a range of altered behaviour including cell proliferation, adaptive protective effects and malignant transformation (Dickey *et al.* 2009; Mothersill & Seymour 1997). This has also been demonstrated to be an effect of senescent conditioned medium (Coppe *et al.* 2008; Dickey *et al.* 2009), and candidates for this effect include IL-8 and IL-6 which are secreted by irradiated senescent cells (Shelton *et al.* 1999; Freund *et al.* 2010).

1.7.5 Senescence in Barrett's oesophagus

The ability of senescent cells to effect neighbouring cells therefore represents a potential mechanism for precancerous cells to affect neighbouring non-senescent cells, or vice versa in the context of Barrett's oesophagus. How abundant is senescence in Barrett's oesophagus? This remains an understudied area. SA β-galactosidase staining of frozen Barrett's samples has demonstrated that there is a consistent upregulation in non-dysplastic, low and high grade dysplastic Barrett's epithelium with lower levels seen when adenocarcinoma develops (Going *et al.* 2002). This is despite the prevailing view that p16 expression loss may occur in metaplasia (Hardie *et al.* 2005) and therefore Barrett's progression may be related to an escape from senescence. A reconciliation of these views may be the upregulation of the alternative senescence pathway, p21 of which there is some evidence. Immunohistochemical analysis by Hanas *et al.* has demonstrated that there is a significant p21 expression from low grade dysplasia which is maintained to adenocarcinoma (Hanas *et al.* 1999). Thus far the relative contributions of p21 and p16 in Barrett's progression have not been studied.

Barrett's oesophagus occurs in the context of a toxic environment (Menges *et al.* 2001) constituents of which are able to induce DNA damage(Clemons *et al.* 2007) which is a potent up-regulator of senescence (Rodier *et al.* 2009). If secreted senescence associated proteins can be protumorigenic then it is possible that clonal populations better able to take advantage of such signals may progress through the metaplasia dysplasia cancer pathway more quickly than others in a genetically

heterogeneous population. As such, abrogation of a senescence response may be a worthy target to prevent subclonal progression.

1.8 Current therapies for Barrett's related cancer and dysplasia

As mentioned in section 1.6.4, understanding field cancerisation as a spread of a clonal epithelial population in the polyclonal environment of Barrett's has several clinical implications not least of which is an understanding of the effects of eradicating clonal populations using endoscopic therapy on a Barrett's segment. Until relatively recently, the only therapy offered for BO was medical (largely with proton pump inhibitors) with decreasing intervals between endoscopies for everything up to high grade dysplasia (HGD) (British Society of Gastroenterology 2005 guidelines (www.bsg.org.uk)) , or surgical therapy for cancer ,and endoscopic therapy had little or no established role. Proton pump inhibitors (PPI) alone can be effective in reducing the rate of progression to cancer (Hillman *et al.* 2004) and can cause regression of dysplasia in some but by no means all cases (Heath *et al.* 2007) . Surgery with curative intent is associated with high rates of mortality and morbidity (Tan *et al.* 1999; Müller *et al.* 1990; Matthews *et al.* 1986). Thus a niche has evolved for other non-surgical therapies particularly in the treatment of dysplastic BO. Endoscopic therapy is of particular interest because the oesophagus is left intact and *in situ* with obvious benefits to the patient. However, given the concept of field cancerization, does endoscopic therapy remove macroscopically abnormal tissue only, or is it successful at removing the clonal populations that are presumed to cause dysplasia? Further, how does endoscopic therapy change the demographics of clonal populations in this polyclonal lesion in a manner that has already been

established in haematological malignancies (Landau *et al.* 2013) and can endoscopic therapies possibly negatively affect outcome?

1.8.1 Types of endoscopic therapy

Endoscopic therapy can largely be subdivided into ablation and non-ablation techniques. Ablation techniques consist of cryotherapy, laser ablation, photodynamic therapy (PDT) and radiofrequency ablation (RFA). These seek to destroy tissue and cannot retrieve samples for histological analysis. Non-ablation techniques include endoscopic mucosal resection (EMR) and endoscopic submucosal dissection and seek to remove rather than destroy tissue so that it can be analysed histologically. The therapies can also be divided according to whether they are focal- so that they are treating a specific area of concern, or field therapies which destroy the area of concern and the Barrett's tissue. Focal and field therapies can be combined as can the different modes of therapy. Different types of ablation therapy exist. These include argon plasma coagulation (APC), laser therapy cryotherapy and photodynamic therapy**.** Although these three have been used previously, and are still occasionally used now, the mainstay of endoscopic therapy is RFA because of the lower complication and higher success rate and therefore this introduction discusses this modality specifically.

1.8.1.1 Radiofrequency ablation

RFA involves the delivery of diathermy energy through either a balloon which will deliver the energy in a circumferential fashion, or *via* a focal probe. The energy is

delivered at 10 to 12 J/cm^2 to produce a depth of damage of around 700 µm which corresponds to destruction of the mucosa without destruction of the submucosa so that the complications of ablation such as bleeding fibrosis and stricturing are less of a concern (Fleischer & Sharma 2008). The burnt tissue (called the coagulum) is then scraped off to ensure that RFA has been adequately and equally applied.

The first multicentre trial performed 1-2 sessions of circumferential RFA in 100 non-randomized patients with CLO only. They were followed up for a period of 1 year during which 70% had complete remission of BO (Sharma*et al.* 2007). The addition of focal ablation to circumferential seemed to improve this figure to 98% remission of BO in 62 patients who underwent surveillance after an initial session of circumferential RFA for 2.5 years (Fleischer *et al.* 2008). RFA was also studied in 142 patients with BO HGD. At 1 year follow-up, complete remission of HGD was achieved in 90.2%, complete remission of dysplasia in 80.4%, and complete remission of CLO in 54.3% of patients (Ganz *et al.* 2008).

In the largest randomised, controlled trial to date, patients with CLO, LGD, HGD and IMC were treated either with up to four sessions of RFA or with a sham procedure. Complete eradication of intestinal metaplasia rates were significantly higher in patients undergoing RFA than sham procedures: 73.8% and 81.0% for HGD and LGD respectively. Overall 77.4% of patients had complete eradication of CLO. Furthermore, less patients progressed in the RFA group (3.6% ablation vs. 16.3%) and there were less subsequent cancers in the treatment arm (1.2% ablation vs. 9.3% control) (Shaheen *et al.* 2009).

A combination of modalities for HGD may prove more effective yet. For visible lesions, EMR followed by RFA of residual BO tissue has resulted in 98% eradication of dysplasia with no recurrence in patients with successful eradication after a 21 month follow-up (R. Pouw *et al.* 2008). Interestingly rigorous biopsy evaluation of the neo-squamous epithelium in a group of 22 post-RFA patients with baseline BO with IMC or HGD showed no evidence of persistent genetic abnormalities or buried BO crypts (Pouw *et al.* 2009).

1.8.2 Methods of assessing success: ablation endpoints

1.8.2.1 The definition of successful endoscopic treatment depends on the treatment intention.

The defined endpoints of ablation therapy vary between clinical trials with various studies quoting successful eradication of IMC rates, or eradication of dysplasia, or eradication to a squamous lining(Fleischeret al. 2008; Shaheen et al. 2011; Shaheen et al. 2009). Strong arguments exist for eradication to a squamous lining being the most effective clinical endpoint.

In a study of factors implicated in recurrence of dysplasia after ablation, persistent Barrett's metaplasia was deemed to be a significant risk (Badreddine *et al.* 2010). In fact residual non-buried BO may carry the same genetic abnormalities found in the HGD indicating that although there is a lower risk of progression as defined by histological grade, there is still the potential for progression (Krishnadath *et al.* 2000). That the intention of ablation has not always been defined as an intention to

eradicate all Barrett's mucosa has led to some confusion in defining poor responders versus those in whom true recurrence is seen. As an example, a trial examining ablation of HGD may present data as eradication of HGD with follow-up data showing its recurrence. If the HGD was only eradicated to LGD or even to columnar lined oesophagus, then that could be interpreted as a poor response rather than recurrence as in fact the main predisposing factor to progression was itself insufficiently eradicated.

Examination of complete eradication of CLO rates rather than intention to treat outcomes, reveals less impressive therapy success rates. In one study, cryotherapy demonstrated a complete CLO eradication rate in 6 out of 30 patients only (J. Dumot *et al.* 2009). In another trial, PDT managed complete CLO eradication in only 33% of those with intramucosal carcinomas- possibly a group of patients who most need complete CLO ablation (Overholt *et al.* 2003). RFA in various trials manages complete CLO eradication in 54 to 79% (Sharma et al 2007; Ganz *et al.* 2008; Shaheen *et al.* 2009; Herrero *et al.* 2011). The most impressive CLO ablation rates are in fact with a combination of modalities such as EMR for visible lesions followed by RFA (Pouw *et al.* 2008).

1.8.2.2 Treatment efficiency over time

Even in patients with complete eradication of non-dysplastic Barrett's oesophagus, there is an appreciable recurrence rate for Barrett's and dysplasia. The initial regrowth after therapy may be squamous and although the time of re-conversion to columnar epithelium is unknown, if we assume it to be similar to the pathway that untreated BO follows, it can take several years (Hamilton &Yardley 1977). The

progression of CLO to LGD may also take a number of years (McCallum *et al.* 1990) and assuming that LGD is always progressive, which itself is contentious, this may also take some time (Peters *et al.* 1999; Hameeteman *et al.* 1989; Miros *et al.* 1991). Furthermore, longitudinal studies estimate of the progression of HGD to cancer may take 24 months on average with a range of 6 to 43 months (Hameeteman *et al.* 1989)(Peters *et al.* 1999). As an example ,in one PDT trial 4 patients whose original histology had shown IMC, and who had a complete remission as defined by absence of cancer or dysplasia, had a recurrence of cancer within 12 months, but a further 6 were noted by 48 months (Pech *et al.* 2005). Patients who have undergone RFA also have an appreciable recurrence rate which becomes evident after 3 years even with repeated RFA therapy (Shaheen *et al.* 2011). Thus the follow-up time to define success is crucial to establish reliable recurrence rates.

1.8.2.3 Why does endoscopic treatment fail?

Although most trials concentrate on positive outcomes such as treatment success, an interesting question is why treatment fails in a patient. There are four possible causes of this:

1.8.2.3.1 Therapy has not targeted the affected tissue

Ablation therapy cannot always guarantee to ablate all Barrett's tissue successfully even with circumferential modalities as can be performed with RFA. In the AIM-2 study 21 of 69 patients (30%) who had undergone an average of 1.5 sessions of circumferential RFA still had evidence of intestinal metaplasia and had to undergo

further focal ablation (Fleischer *et al.* 2007). Residual tissue has also been found with other ablation modalities and can be interpreted as the percentage who of patients who did not achieve a complete eradication of intestinal metaplasia.The persistence of non-buried Barrett's may relate to the operator's application of the ablation being inadequate or the technique itself missing the target. Circumferential RFA may not adequately ablate BO at the gastro-oesophageal junction for example. A third reason may be related to mucosal penetration. Assuming BO to be a disease solely of the mucosa- and this is itself contentious- the depth of ablation should be at least that of the depth of the mucosa. This has to be balanced against the risk of complications caused by necrosis and fibrosis of the submucosa. BO has an average depth of 0.6mm (Ackroyd *et al.* 1999) . RFA typically penetrates to a depth of 0.7mm. PDT can produce tissue necrosis up to a depth of 6mm which may account for its high stricture rate (Chatlani *et al.* 1991; Heier *et al.* 1995). Laser therapy can produce a depth of necrosis between 3-4 mm with the Nd:YAG laser to 1 mm with the argon lasers (van den Boogert *et al.* 1999) and cryoablation can reach a depth of 2mm (Johnston *et al.* 2005) . Clearly therefore all should be able to eliminate all Barrett's mucosa. The fact that this is not the case may relate either to the variability of the thickness of Barrett's mucosa- the average is 0.6mm but can be as deep as 1.3mm (Chandrasoma & Wikramasinghe 2003) - or to the ablation technique having difficulty accessing the source of the Barrett's tissue.

1.8.2.3.2 The pathology is hidden

The persistence of somatic mutations thought to contribute to BO progression has been detected after PDT in 2 out of 3 patients who had an initial downstaging of their HGD after the therapy but in whom HGD recurred within the 12 month follow-up (Krishnadath *et al.* 2000). Persistence has also been noted after RFA (Finkelstein & Lyday 2008) . In this study the persistent mutation was noted in only 1 patient out of 16 who was refractory to treatment. This persistence of genetic phenomena suggests the persistence of a clonogenic cell that can cause dysplasia to recur and suggests that the treatment has not adequately ablated this clonogenic source. Apart from the fact that ablation has not have been properly applied, this may be due to the clonogenic source being effectively protected from diathermy.

Buried BO relates to the presence of columnar lined epithelium situated beneath squamous tissue. This is thought to arise as a result of the overgrowth of neo-squamous islands (NSE). NSE is oesophageal tissue that has regenerated following treatment for BO. It is common and seen in up to 77% of BO patients after treatment with PPIs (Ban *et al.* 2004)(Sampliner & Fass 1993) with higher figures after ablation and reaching 100% in patients treated with PDT (Ban *et al.* 2004)(Biddlestone *et al.* 1998).

NSE may develop as a spectrum from a complete replacement of Barrett's tissue to distinct islands of differing sizes. The extent of development also depends on the type of treatment. Patients treated with RFA for example will develop complete replacement of Barrett's mucosa with NSE in almost all cases(Sharma, Wang, et al. 2007; Sharma, et al. 2007; Gondrie et al. 2008). NSE is phenotypically the same as

normal oesophageal squamous tissue and genotypically is usually normal suggesting that the multipotential cell of origin for NSE and normal squamous tissue is likely to be the same and different to the origin of BO. This is particularly so as it has been shown that NSE surrounded by Barrett's tissue shares usually none of the BO associated mutations (Paulson, LJ Xu, et al. 2006; Leedham et al. 2008). However more recent evidence has demonstrated a mitochondrial DNA mutation common to both the squamous and neighbouring Barrett's epithelium suggesting that the two may indeed have a common stem cell origin (Nicholson *et al.* 2011).

1.8.2.3.3 Buried Barrett's

The presence of buried Barrett's depends on the treatment technique being used. After PPI use, buried Barrett's and buried dysplasia can be found in as many as 27% and 12.1% of patients respectively and increases to 51% and 27.3% respectively after PDT (Ban *et al.* 2004). RFA on the other hand does not seem to cause buried Barrett's in almost 100% of patients (Sharma*et al.* 2007; Gondrie *et al.* 2008; Gossner *et al.* 1988) although more recent studies refute this (Zhou *et al.* 2012).

Although buried Barrett's is pathologically similar to pre-treatment BO, the main concern is with the development of dysplasia in an area that is hidden from the endoscopist's view. The development of adenocarcinoma in such cases has been described (Sampliner & Fass 1993; Van Laethem *et al.* 2000; Reid *et al.* 2000). Despite this, the buried dysplasia found after treatment may be less aggressive than untreated dysplasia. Evaluation of the biological properties of buried dysplasia after PDT for example has shown a lower crypt proliferation rate and lower DNA content

abnormalities as measured by image cytometry, as compared with pre-treatment Barrett's oesophagus (Hornick *et al.* 2008). It has been suggested that the lack of connection of the buried areas to the luminal surface may protect it from the further damage needed for progression.

1.8.2.3.4 The dysplastic stem cell is in the submucosa

Another issue relates to whether the cell of origin of a BO is being adequately eradicated by the ablation method; this is itself a question of where the origin of Barrett's tissue lies. The origin of metaplasia has not been firmly established and there remain several theories. Initially BO was thought to arise from the stomach based on the fact that it is commonly found in the distal oesophagus confluent with the gastro-oesophageal junction, it progresses upwards over time, and it shares a similar morphology to the stomach (columnar epithelium). Using jejunal interposition grafts between the stomach and oesophagus in canine models, it can be shown, after acid stimulation, that columnar epithelialisation can still occur, demonstrating that the origin of Barrett's mucosa may not be from the stomach (Gillen *et al.* 1988); despite this considerable evidence exists that a gastric source may be implicated (see section 1.4.1). Furthermore, gastric type mucosa can be found in the proximal oesophagus without connection to the stomach as found in the cervical inlet patch (Malhi-Chowla *et al.* 2000).

A second theory suggests that the metaplastic change arises from the proposed oesophageal stem cells located at the bottom of the interpapillary region of the oesophageal epithelium (Seery & Watt 2000) (see section 1.4.4). This area was found

to proliferate rarely and when it does, it results in an asymmetric mitosis resulting in one daughter and one parent cell. This was, until recently, thought to be characteristic of stem cell compartments in other tissues but more recent evidence has demonstrated this may not be the case (Snippert *et al.* 2010). If the source of dysplasia was in this area, ablation would have direct access to the tissue as long as the depth of therapy was at least equal to the depth of the epithelium (Jones *et al.* 2005).

A third theory suggests that the metaplastic change arises from cells located in the submucosal layer, such as oesophageal submucosal gland ducts, which are located throughout the oesophagus but more concentrated distally. The finding of a common mutation between a duct cell and the overlying Barrett's mucosa supports this theory although most NSE is wild-type (Paulson *et al.* 2006) (Leedham *et al.* 2008). If the submucosal duct cell is the origin, then theoretically most ablation methods, which produce injury only within the mucosa, would be unable to reach the potentially mutated BO founder cell in the submucosal duct. In fact on the basis of the clinical trials above, RFA seems to have the best outcome for ablation of dysplastic epithelium with NSE regrowth for the follow-up times measured suggesting that either RFA does reach the submucosa or that the dysplastic clone is more superficial.

1.8.2.3.5 The tissue has ablation resistant mutations

The progression of Barrett's mucosa from metaplasia through to dysplasia and cancer is associated with a variety of somatic mutations and other genetic and

epigenetic events (Fitzgerald 2006). Initial evidence pointed to a field cancerization model of BO in which a genetic mutation was disseminated through the oesophagus through as yet undescribed mechanisms but is probably a form of crypt fission (discussed in section 0). This field then acted as a permissive area for further mutations to develop which themselves spread and so on, causing phenotypic changes and eventually cancer. This model may have been based on experimental artefact and more recent evidence based on exhaustive microdissection of Barrett's tissue has demonstrated that the mucosa is made up of cells with a number of different mutations indicating a variety of clones (Leedham*et al.* 2008). Some of the most common somatic mutations are associated with crucial cell cycle control events (*CDNK2A*)(Klump *et al.* 1998; Paulson *et al.* 2008b), or regulation of apoptosis (*TP53*) (Galipeau *et al.* 1999). *TP53* in particular is important in a number of human cancers and has been found to be mutated with increasing frequency as BO progresses towards adenocarcinoma (Dolan *et al.* 2003). Because of its central role in causing apoptosis in damaged cells, lack of functional p53 can render a cell more resistant to apoptosis and therefore more susceptible to genomic damage and the acquisition of further mutations. Mouse experiments have demonstrated increased survival to γ-irradiation or chemotherapy if the transgenic mouse expresses mutant trp53 (the murine equivalent to *TP53* in humans) (Lee & Bernstein 1993). Furthermore in humans patients with breast cancer, cells with *TP53* mutations demonstrate resistance to doxirubicin treatment and early relapse (Aas &*et al.* 1996). This resistance, depending on the mutation, has been found to extend to such diverse insults as heat (Ota *et al.* 2000). It is conceivable therefore those certain genetic or

epigenetic mutations confer a resistance to ablation type damage and therefore are likely to persist.

1.8.2.3.6 The conditions persist after BO treatment

Some patients will continue to have evidence of reflux after ablation therapy despite also being on a PPI. Arguably subsequent changes in the mucosa after squamous regrowth may be attributable to the on-going presence of gastro-oesophageal reflux disease (GORD). Certainly the risk factors for recurrent dysplasia after RFA are similar to the aetiology of GORD (Badreddine *et al.* 2010) and studies demonstrating insufficient acid suppression suggest metaplasia and dysplasia is more difficult to control (Overholt 2000). There is evidence that PPI therapy after thermal ablation, for example, significantly reduces the risk of recurrent Barrett's epithelium, and that this is related to normalisation of pH (Van Laethem *et al.* 1998; Schulz *et al.* 2000; Kahaleh *et al.* 2002). In such a scenario one would expect that if ablation was successful, squamous regrowth would completely cover the previous Barrett's mucosa. If the BO returns and is due to GORD then the regrowth would most likely to be due to a different clonal cell population to the original Barrett's epithelium.Studies analysing genetic mutations before treatment and in the rare instance after a recurrence when the intervening mucosa was neo-squamous have not been done, presumably because such patients are difficult to find.

1.8.2.3.7 The Barrett's tissue recurs post treatment

As discussed in section 1.8 there is a recurrence rate after the endoscopic treatment of BO. Recurrent dysplasia could occur for any of the reasons mentioned in section 1.8.2.3, but a further possibility remains. Haematological malignancies have documented a change in subclonal structure after chemotherapy such that previously non dominant clonal populations proliferate after the eradication of dominant clonal populations (Obermann *et al.* 2011; Landau *et al.* 2013). Although this has not been described in solid organ malignancies presumably because of difficulties of longitudinal and geographic sampling of such malignancies, it remains a possible explanation for recrudescence of dysplasia after eradication to a non-dysplastic BO.

Hypotheses

The introduction has described BO as a polyclonal premalignant lesion. Clonal lesions in BO expand through a process of field cancerization the underlying mechanism of which is as yet undescribed. The fact that BO is polyclonal raises the possibility that clonal interactions are responsible for field cancerization and adenocarcinoma progression although the mechanism for clonal interactions has not been elucidated- one possible interaction is the senescence associated secretory pathway.

My hypotheses are therefore

1) That clonal interactions exist between clonal populations and may drive carcinogenesis.
2) That a potential mechanism by which clonal interactions occur is through senescence and its associated secretory phenotype.
3) That clonal populations can persist to cause cancer despite endoscopic ablation therapy.

1.9 Aims

To determine the clonal relationships between premalignant Barrett's and cancer by:

i) Comparing the mutational status of dysplastic Barrett's with its related adenocarcinoma.
ii) Demonstrating the spatial relationships between clonal populations in pre-cancerous Barrett's.

To determine the role of senescence as a mechanism for clonal interaction by:

iii) Assessment of the presence of senescence in pre-malignant and malignant Barrett's oesophagus by analysis of expression of p21 and p16.

iv) Establishing an in vitro model of cellular senescence and using this model to assess the effects of senescent cells on neighbouring, non-senescent cells.

v) Assessment of whether senescent cells in malignant and premalignant Barrett's oesophagus also secrete factors associated with the senescent associated secretory phenotype.

vi) Assessment of whether the expression of p16 as a senescent marker is also a marker of a clonally derived cell population.

To determine the clonality of pre and post ablation Barrett's related pathology by:

vii) Examining a case series of patients who have undergone RFA and EMR and understand the clonal correlates of persistent or recurrent HGD or OAC in patients undergoing endoscopic therapy.

viii) Establishing the potential reasons why clonal cancer associated cell populations may be persistent despite treatment with ablation therapy.

Chapter 2 Materials and Methods

2.1 Patients

2.1.1 Assessment of the clonality of premalignant Barrett's oesophagus as compared with its associated malignancy

Tissue was obtained retrospectively from Gloucestershire Royal Hospital and University College London Hospital (UCLH). All tissue had been retrieved for clinical indications and was formalin fixed and paraffin embedded (FFPE). The tissue included biopsies, endoscopic resections and oesophagectomies from patients with high grade dysplasia or adenocarcinoma.Access to human tissue was available through the ethical procedures of the Multicentre Research Ethics Committee. (MREC 07/Q1604/17) and Multicentre Research Ethics Committee (11/LO/1613).

2.1.2 Clonal selection after endoscopic therapy of Barrett's related high grade dysplasia and adenocarcinoma

All tissue was obtained from University College London Hospital (UCLH) and was formalin fixed and paraffin embedded. Samples were obtained retrospectively from an archive kept at UCLH and had been taken specifically for clinical reasons. Patients who had undergone RFA were identified from the RFA registry at UCLH and samples before and after courses of RFA were taken.Only patients with recurrent or persistent disease after RFA and/or endoscopic mucosal resection (EMR) of HGD or

intramucosal adenocarcinoma (IMC) were chosen for analysis. Furthermore, patients had to have undergone two further endoscopic samplings subsequent to the initial ablation therapy.Access to human tissue was available through the ethical procedures of the Multicentre Research Ethics Committee. (11/LO/1613).

2.1.3 Histological scoring of CXCL1 (GROα) and CCL5 (RANTES)

All tissue was obtained from a histopathological archive at UCLH and was formalin fixed and paraffin embedded. All tissue was comprised of either endoscopic mucosal resection or biopsies and had been taken for clinical reasons. Access to human tissue was available through the ethical procedures of the Multicentre Research Ethics Committee. (11/LO/1613).

2.2 *Ex vivo* tissue preparation and processing methods

2.2.1 Tissue preparation

All laser capture was performed on FFPE tissue. PALM laser capture slides (P.A.L.M. Microlaser technologies, GmbH, Germany) were prepared by exposure to ultraviolet light at 254mm wavelength for 30 minutes. Each FFPE block underwent sectioning into 7 sections at 6 µm thickness. The first section was cut onto a frosted glass slide (Colorfrost, Thermo Fisher Scientific,Loughborough, UK) and was stained for haematoxylin and eosin (see methods 0). The subsequent 6 sections were cut serial to the initial slide onto the ultraviolet treated PALM slides (P.A.L.M. Microlaser technologies, Germany), and the slides were numbered accordingly.

2.2.2 Methylene green staining

Methylene green staining provides adequate differentiation of the crypts from the surrounding stroma and does not affect subsequent PCR. Sections on PALM laser capture slides (P.A.L.M. Microlaser technologies, Germany) were dewaxed in xylene, and rehydrated in decreasing concentrations of ethanol.Each PALM laser capture slide (P.A.L.M. Microlaser technologies, GmbH, Germany) then underwent immersion in methylene green stain for 20 seconds (Sigma-Aldrich, UK) followed by gentle rinsing in tap water. They were then left to air dry for thirty minutes.

2.2.3 Laser capture microdissection

Laser capture allows the capture of distinct cell populations from heterogeneous tissue samples. The laser capture device used throughout this thesis was an ultraviolet laser (P.A.L.M Microlaser Technologies, GmbH, Germany). After visualisation of methylene green stained tissue under white light microscopy, the laser capture device photo-volatises a user-defined specific area of tissue and catapults it into a collecting tube using a ultraviolet laser pulse.

Crypts for dissection were identified on the H&E slide and followed through the six serial, methylene green stained sections. Individual crypts were cut from the six serial laser capture slides and catapulted into the adhesive caps of eppendorfs using the P.A.L.M. Laser Microdissection system(P.A.L.M Microlaser Technologies, Germany). This dissected sample was immersed in 12 µl of proteinase K solution (Arcturus Bioscience, Mt View, California, USA). 12 µl proteinase K solution and no laser capture material was used as a negative control tube. Tubes were then

centrifuged at 4.5 g for 1 min and incubated at 65°C overnight. A 10 min incubation at 95°C denatured the proteinase K and the lysate was then stored at -20°C.

2.2.4 Haematoxylin & eosin staining

6µm FFPE sections were mounted onto frosted glass slides (Colorfrost, Thermo Fisher Scientific, UK) and were immersed in Gill's haematoxylin (Pioneer Research Chemicals, UK) for 4 minutes and eosin (Pioneer Research Chemicals, UK) for 3-5 minutes. The slides were then washed in tap water and dipped in acid alcohol (1% v/v concentrated hydrochloric acid in 70% alcohol) (Sigma-Aldrich, UK). They then underwent a further wash in tap water before dehydration through graded alcohols to xylene (BDH, Poole, UK) and mounted in DPX (Sigma-Aldrich, UK).

2.3 Cell culture techniques.

2.3.1 Growth of cell lines and cell line assays

Cell culture media for individual cell lines are listed below. All reagents were pre-heated to 37°C before use. The medium was changed every 3 days for all cultures unless otherwise stated.

Cell line	*Culture Media*	*Tissue grade*	*Provided by*
BAR-T	Keratinocyte Growth Medium BPE (bovine pituitary extract). hEGF. Insulin (recombinant human). Hydrocortisone. GA-1000 (gentamicin, amphotericin B). (All constituents are from Lonza, Switzerland- constituent concentrations are confidential).	Non-dysplastic	Rhonda Souza, UT Southwestern Medical Centre
OE33	RPMI-1640 (PAA, Yeovil, UK) 10% Heat inactivated foetal calf serum (Invitrogen Life Technologies, UK), 1% penicillin-streptomycin (PAA, UK)	Cancer	Rebecca Fitzgerald, MRC Cancer Cell Unit, Cambridge
GoTERT	MCDB-153(Sigma-Aldrich,UK) 0.4 µg/ml hydrocortisone (Sigma-Aldrich,UK) 20 ng/ml recombinant human EGF (Epidermal Growth Factor) (Sigma-Aldrich,UK) 1 nM cholera toxin (Sigma-Aldrich,UK) 20 mg/L adenine (Sigma-Aldrich,UK) 140 µg/ml BPE (Bovine Pituitary Extract) (Sigma-Aldrich,UK) 0.1% ITS [Insulin-Transferrin-Sodium Selenite Supplement (Sigma-Aldrich,UK) 4 mM glutamine (Sigma-Aldrich,UK) Foetal bovine serum to a final concentration of 5% (Invitrogen Life Technologies, UK)	Dysplasia	Rebecca Fitzgerald, MRC Cancer Cell Unit, Cambridge
Phoenix A	Dulbecco's modified Eagle medium (Invitrogen, UK) 10% Heat inactivated foetal calf serum (Invitrogen Life Technologies, UK), 1% penicillin-streptomycin (PAA, UK) Glutamine 2mM Invitrogen,UK).	Kidney epithelium	Ken Parkinson, Centre for Diagnostic and Oral Sciences, Blizard Institute, London

Table 2-1: Cell lines and associated growth media used.

2.3.1.1 Sub culturing cells

Cells cultured cells in 25 cm^2 flasks (BD Falcon, Oxford, UK) were washed twice by pipetting 15ml of sterile PBS (PAA, UK) over the cells and then pipetting the PBS out. 4ml of 1X trypsin (GE Healthcare, Buckinghamshire, UK) preheated at 37°C was then added to the flask and rocked so that it covered all the cells. This was then incubated at 37°C for two minutes. The cells were encouraged to detach by gently knocking the bottom of the flask. Media containing 10% foetal bovine serum (FBS; Invitrogen Life Technologies, UK) was then added and then cells removed by pipetting into a 50ml Falcon. They were washed twice by centrifugation at 1 $x10^3$rpm for 5 minutes followed by exchange of PBS and then after the final wash, the PBS was exchanged for 15ml of culture media and the cells counted and plated accordingly so that 1 $x10^6$ cells were placed in a new 25cm^2 flask. Cells that were not needed were either frozen as described (methods 2.3.1.3) or discarded.

BAR-T cells require collagen coating of plates in order to proliferate. Human collagen IV (BD Biosciences) stored at -20°C was thawed and diluted to 10µg/ml using 10mM acetic acid (Sigma-Aldrich,UK) so that the final coating concentration was 1.0µg/cm^2. This was then incubated for 1 hour at room temperature and remaining material was aspirated. Once the dishes had been rinsed carefully to remove remaining acid they were ready for use.

2.3.1.2 Thawing frozen cells

Cells stored in liquid nitrogen were quickly thawed by immersion of the containing cryovial in tap water at 37°C. The cells were pipetted out and placed in a falcon with 5ml of warm PBS and centrifuged at 1 $x10^3$ rpm for 5 minutes. The PBS was

exchanged for 5ml of warm RPMI-1640 (PAA, UK) and underwent further centrifugation for 5 minutes at 1 x10^3 rpm. The RPMI-1640 was exchanged for fresh culture media and cells were counted as described (see section 2.3.1.4) prior to plating on a tissue culture flask or plate.

2.3.1.3 Freezing live cells for storage

Cells were trypsinised as described previously (see section 2.3.1.1). Following neutralisation with serum containing media, the cells were centrifuged in a 50ml falcon tube at 1 x10^3rpm for 5 minutes. The media was then replaced with PBS and cells re-suspended for a further 5 minutes centrifugation at 1 x10^3rpm. The cells were then re-suspended at a concentration of ~1 x 10^6cells/ml in FBS (Invitrogen Life Technologies, UK) to which dimethylsulphoxide (DMSO; Sigma-Aldrich, UK) was added to a final concentration of 10% (v/v) and transferred into 2 ml cryovials. Cryovials were stored in a cryochamber containing isolpropanol (Thermo Fisher Scientific, UK) and slowly cooled to -70°C for at least 4 hours. The samples were then transferred to liquid nitrogen.

2.3.1.4 Determination of cell concentration and viability

Cell viability was assessed by trypan blue exclusion assay after trypsin digestion and neutralisation with the appropriate media for the cell type containing 10% FBS (Invitrogen,UK). 50µl of the cell suspension was mixed with 50µl of trypan blue (0.4% w/v) (Sigma-Aldrich, UK). Non-viable cells stain blue, viable cells are clear. A drop of the cell suspension was placed between a coverslip and a haemocytometer and examined using a phase contrast microscope (Nikon Eclipse TE2000-S inverted

microscope, Nikon, Japan). The cells were counted in all four large squares and the number of cells/ml calculated. Viability was determined by counting the proportion of cells that stain blue compared to the total number of cells counted and expressed as a percentage.

2.3.1.5 Irradiation of cells

Cells were initially seeded in 6,12,24 or 96 well plates depending on the experiment, at the appropriate seeding density in media appropriate to the cell type (see

Table 2-1) and incubated at 37°C, 5% CO_2 overnight. 24 hours after seeding the cells were then submitted to caesium gamma irradiation (Gamma Service Irradiator D1, Gamma Service Medical, Leipzig, Germany) at the determined Gray. The cells were then placed in an incubator at 37°C 5% CO_2. Media and dead cells were removed every 2 days prior to experiments being performed at the determined day.

2.3.1.6 Colony formation assay

Colorimetry consisted of removal of media from each well seeded with cells and fixation with 4% paraformaldehyde (Sigma-Aldrich, UK) for 20 minutes. This was washed off with PBS (PAA,UK), and 0.05% crystal violet (Sigma-Aldrich, UK) was added for a further 5 minutes. This was washed off with tap water. Methanol (Thermo Fisher Scientific, UK) was then added to each well to solubilize the crystal violet and submitted to a plate reader (Victor, PerkinElmer, MA) for analysis at an absorbance of 450nm.

2.3.1.7 MTT assay

After a specified number of days cells seeded in 96 well plates underwent MTT assay (Vibrant assay, Sigma-Aldrich, UK) to assess proliferation. Accordingly, cell media was removed and washed with PBS. 100µl of RPMI-1640 with no phenol red (PAA, UK) was then placed in each well and 10µl of MTT (Sigma-Aldrich, UK) was added. Cells were then incubated for 4 hours at which time 75µl of the incubating media was removed and DMSO (Sigma-Aldrich, UK) added. This was incubated for 10 minutes and then submitted to a plate reader at 540nm absorbance for colorimetric analysis (Victor, PerkinElmer, Waltham, MA).

2.3.1.8 SA β-Galactosidase assay

SA β-galactosidase is a commonly used marker of senescence used to detect lysosomal β-D-galactosidase, encoded for by the gene galactosidase β-1 (GLB1)(Lee *et al.* 2006). The senescence response involves an expansion of the cellular lysosomal compartment with a subsequent upregulation of lysosomal β-D-galactosidase although the enzyme is not thought to take part in the senescence response (Lee 2006). Nonsenescent cells can display SA β-galactosidase activity in the lysosomes that functions most optimally at pH 4.0 (Lee *et al.* 2006). Because of the increased lysosomal compartment in senescent cells, SA β-galactosidase becomes detectable at suboptimal pH 6.0(Dimri *et al.* 1995).

At the specified day after seeding in a 6 or 12 well plate, all media was removed from cells which were then fixed in 4% paraformaldehyde (Sigma-Aldrich, UK) for 5 minutes at room temperature. This was then thoroughly washed off with PBS (PAA, UK) and SA β-Galactosidase staining solution (Sigma-Aldrich, Poole, UK) addedtoeach

well. The cells were then incubated at 37°C atmospheric CO_2. After 6 hours, the staining solution was washed off three times with PBS (PAA, UK) and the cells examined using a phase contrast inverted microscope (Nikon Eclipse TE2000-S inverted microscope, Nikon, Japan). SA β-galactosidase positive and negative cells were counted in 5 random fields of view per well, in triplicate. Randomness was achieved by placing a transparent numbered grid over the well cover and generating a random number (using http://www.random.org/) which corresponded to a grid number. The cells were then counted in the chosen grid.

2.3.2 Transfection of cell lines-GFP cell line

2.3.2.1 *pBABE-puro* plasmid source and structure

Infection refers to the introduction of nucleic acids into a cell using a virus. *pBABE-puro*-IRES-EGFP (Addgene, Cambridge, MA) is a commercially available plasmid based on the pBABE series and contains the long terminal repeat (LTR) allowing gene expression, packaging sequences from the *MoMLV-LTR* (Murine Moloney Leukemia Virus). The plasmid contains the green fluorescent protein gene (GFP). Viral replication depends on the presence of env and reverse transcriptase genes which have been deleted in this plasmid rendering the plasmid replication defective.

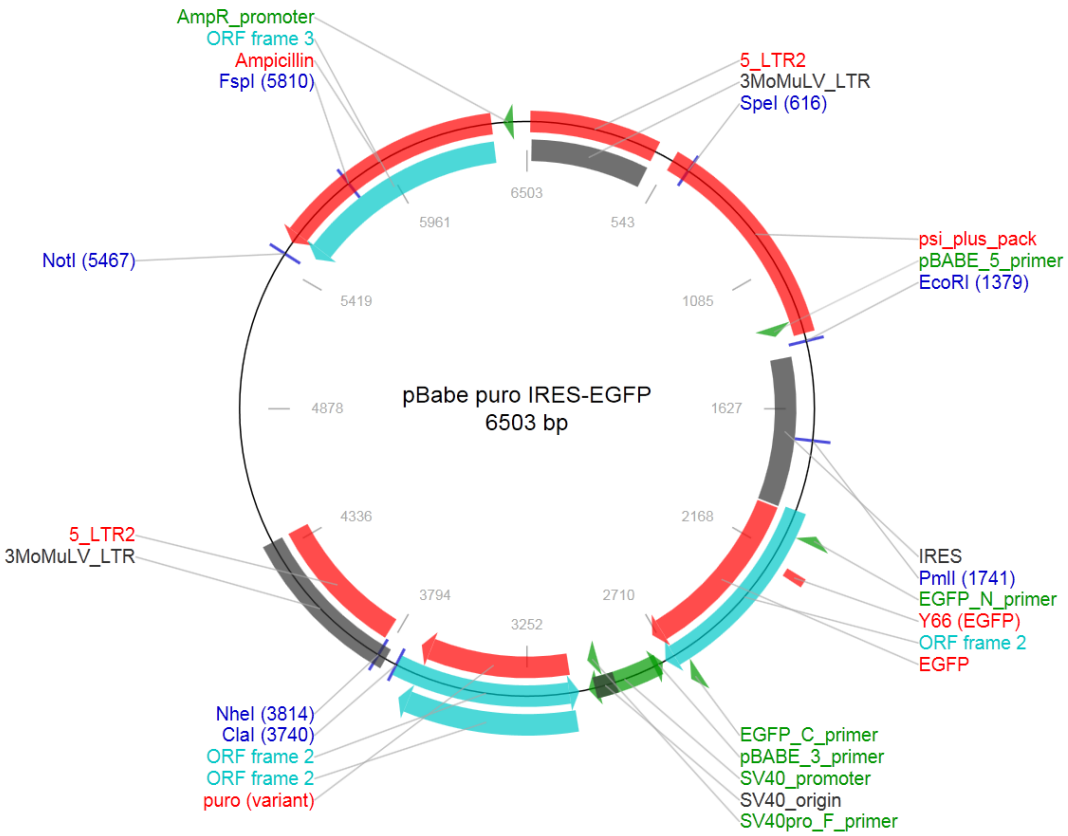

Figure 2-1: PBabepuro Plasmid structure.
Adapted from http://www.addgene.org/browse/sequence/8086/Amplification of High Copy Number pBABE-puro plasmids using competent E.coli *bacteria*

1 µl of the *pBABE-puro*-IRES-EGFP plasmid (Addgene, MA) was mixed with 0.1 ml *E. coli* JM109 competent cells ,which had been pre-treated by the manufacturer to ensure competency (Promega, Madison, WI), in a sterile eppendorf tube on ice and gently mixed by tapping. Competency refers to the ability of a cell to take up genetic material. An eppendorf containing no DNA was also prepared as a control tube. The tubes were then incubated on ice for 20 minutes and then at 42°C for exactly 2 minutes in a circulating water bath. The tubes were then further incubated on ice for 1-2 minutes. 1 ml of Luria-Bertani Broth (LB) medium (Sigma-Aldrich, UK) was then added to the tube and mixed by gentle tumbling. This was then incubated for 60 minutes at 37°C. 200µl was then pipetted onto an agar plate containing 25mg/ml ampicillin (Sigma-Aldrich, UK) and the plate was then incubated overnight at 37°C.Individual colonies were selected with a pipette tip, incubated into LB medium and put on a shaking incubator at 37°C at 200-rpm for 16 hours.

Bacterial cells were harvested by centrifugation at 8000rpm for 3 minutes at room temperature after which supernatant was decanted off. Isolation of the plasmid was performed according to manufacturer's instructions (QIAprep Spin Miniprep, Qiagen, UK). All chemical names and concentrations of constituents are confidential. All spin-columns and microcentrifuge tubes were provided by the manufacturer. Accordingly, the bacterial pellet was resuspended in 250µl of buffer P1 and transferred to a microcentrifuge tube to which 250µl Buffer P2 was added and mixed thoroughly by inverting several times. 350 µl Buffer N3 was then added and the tube again mixed by inverting several times. The tube was then centrifuged for 10 minutes at 13,000

rpm to form a compact white pellet. The supernatant was then decanted onto a QIAprep spin column and centrifuged for 60 seconds; the flow through was then discarded. 0.5ml of Buffer PB was then added to remove trace nuclease activity and centrifuged for 60 seconds. The flow through was then discarded and 0.75ml of Buffer PE added and centrifuged for 60 seconds. Residual wash buffer was removed by discarding the flow through once more and centrifuging the spin column for an additional 1 minute. The spin column was then placed in a clean 1.5ml microcentrifuge tube and the DNA was eluted by addition of 50µl Buffer EB (10mM Tris-Cl, pH 8.5- supplied by manufacturer), letting the column stand for 1 minute and a subsequent final centrifugation for 1 minute. The plasmid concentration was confirmed with using a calculated 260/280nm absorbance ratio in a Nanodrop (Thermo Fisher Scientific, UK).

2.3.2.2 Growth and transfection of phoenix A packaging cells to produce vector particles

Phoenix A cells are derived from the 293T cell line (an embryonic human kidney cell line) and are second-generation retrovirus producer cells. They are highly effective in lipid-based transfection protocols. They contain a construct capable of producing *gag-pol*, and envelope protein for amphotropic viruses and therefore allow plasmid to be packaged inside a virus in order to infect human cells.

$1x10^6$ Phoenix A cells (Invitrogen, Paisley, UK) were seeded in a 60mm dish in 4ml media containing RPMI-1640 (PAA, UK) supplemented with 10% heat inactivated foetal calf serum (Invitrogen Life Technologies, UK) and 1% penicillin-streptomycin (PAA, UK). These were then incubated at 37°C, 5% CO_2 for 24 hours after which the

media was aspirated off and further media added. 100 µl of serum free media was added to a sterile tube and 25 µg Fugene (Promega, UK) was added drop wise to this. This was incubated at room temperature for 5 minutes and 8µg of the plasmid DNA was added. This was incubated for 15 minutes at room temperature and subsequently added to the phoenix A cells. Transfection efficiency was confirmed by assessment of fluorescence using a fluorescent microscope (Nikon Eclipse TE2000-S inverted microscope, Nikon, Japan). 48 hours after transfection, once 75% of the cells were fluorescent, the cells were split into a culture dish with media containing 2µg/ml puromycin (Invitrogen Life Technologies, UK). Dead cells were removed regularly and at 75% confluence the media was removed, washed with PBS and 10ml of serum free media was added. This was then incubated at 32°C overnight and the following morning the virus containing supernatant was removed and centrifuged at $1.5x10^3$ rpm for 5 minutes. This was then snap frozen in liquid nitrogen and stored at -80°C.

2.3.2.3 Infection of OE33 cell line with pBABE-puro plasmid.

OE33 cells were seeded in a 6 well plate at $2x10^5$ cells per well and incubated overnight. Polybrene (Sigma-Aldrich, UK) was added to media to achieve a final concentration of 5µg/ml. To assess infection efficiency, different ratios of virus supernatant to polybrene-media mix (1:2, 1:5, 1:10, 1:20, 1:50, 1:100) were added to the seeded OE33 cells. This was allowed to incubate for 5 minutes at room temperature prior to being washed off with PBS and normal RPMI-1640 (PAA, UK)added.

Fluorescence assessment at day 4 demonstrated a 1:2 ratio to be the most successfully infected and was therefore taken forward for further experiments. Puromycin (Invitrogen Life Technologies, UK) was added to these cells and the dose optimised at 4μg/ml. Infection was continuously monitored until 90% infection efficiency was achieved by observation under a fluorescence microscope (Nikon Eclipse TE2000-S inverted microscope, Nikon, Japan) and confirmation of GFP transfection efficiency was obtained by flow cytometry and comparison with a GFP negative control (Figure 2-2).

2.3.2.4 Single Cell cloning of OE33^{GFP+} cells

To ensure that cells used in further experiments are a clonal population, GFP infected cells were plated in serial dilutions in a 96 well plate (BD Falcon, UK). The wells were examined and the well that contained only one colony was selected for further growth. Once at 90% confluence, the cells in the selected well were trypsinized and grown in serially increasing container sizes.

2.4 Protein analysis methods

2.4.1 Immunohistochemistry and Immunofluorescence

Throughout the thesis, immunohistochemistry was performed using the indirect streptavidin-biotin method. Sections from FFPE cassettes were prepared on frosted glass slides (Colorfrost, Thermo Fisher Scientific, UK) at 6 μm thickness. Sections were dewaxed in xylene, rehydrated in decreasing concentrations of ethanol and incubated with 0.3% hydrogen peroxide (H_2O_2; VWR International, Radnor, PA) for 10 minutes to block for endogenous peroxidase activity.

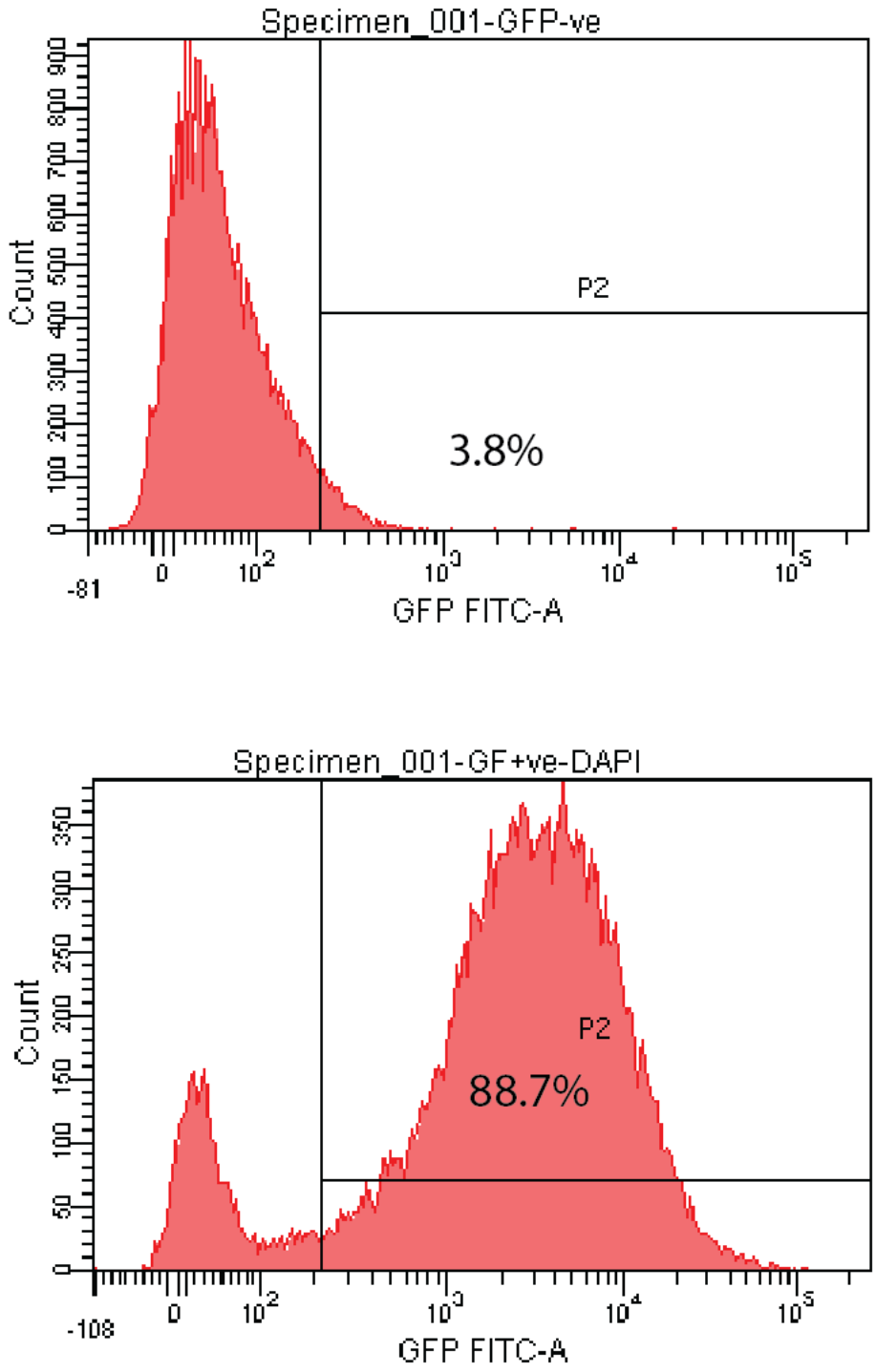

Figure 2-2: Demonstration of proportion of OE33 cells expressing GFP.
The cells have been sorted using flow cytometry based on GFP expression a) Negative control b) GFP positive OE33 cells. P2 represents the proportion of cells expressing GFP.

Protocols for individual antibodies are shown in

Table 2-2. If antigen retrieval was required, it was performed by adding slides to a boiling 0.01M solution of sodium citrate buffer (Sigma-Aldrich, UK) (pH 6.0) and microwaving for 10 minutes. Subsequently, sections were washed and cooled in tap water and then placed in phosphate buffered saline with 0.2% Tween 20 (Sigma-Aldrich, UK). The sections were pre-incubated for 15 minutes in 5% normal serum from the immunised species of the secondary antibody (DAKO, UK) in PBS to reduce the amount of non-specific binding of the antibodies. Sections then underwent incubation in a primary antibody for 30 minutes at room temperature. After 3 washes in PBS for 5 minutes each, sections were incubated with the species-specific biotinylated secondary antibody, diluted in 5% serum in PBS, for 30 minutes before being further washed 3 times at 5 minutes. A tertiary layer of streptavidin-horseradish peroxidase (strep-HRP; DAKO, UK) diluted at 1:500 was then applied. Dilutions of all layers were in PBS. The sections were developed with 3,3-diaminobenzidine-tetrahydrochloride solution (DAB; Sigma-Aldrich, U.K.) for 2–8 minutes, guided by frequent observation under a light microscope, before two 5 minute washes in PBS, rinsing in tap water and counterstaining with Gill's haematoxylin (Pioneer Research Chemicals, Colchester, UK). Sections were then dehydrated through increasing concentrations of alcohol and finally rinsed twice in xylene. DPX (Distyrene, a plasticizer, and xylene; Sigma-Aldrich, UK) was applied to the section and a coverslip applied.

2.4.1.1 Immunofluorescence

Each primary antibody was applied and washed as per section 2.4.1. Each section was then incubated with the relevant secondary antibody conjugated to a fluorescent probe at room temperature for 35 minutes in the dark and then washed 3 times for 5 minutes each in PBS. DAPI hardset (Vector Laboratories, Burlingame, CA) was then applied to the slide and left overnight at 4°C for fluorescence microscopy examination the following day.A separate isotype matched control immunoglobulin (isotype matched immunoglobulin from unimmunised animals) was used at the same concentration as all experimental primary antibodies and included in each staining run.

2.4.2 Enzyme linked immunoabsorbent assay (ELISA)

Each ELISA was carried out using a Multi-analyte kit (Qiagen, UK) and used according to manufacturer's instructions. This allows the detection of several chemokines simultaneously (Interleukin 8 (IL-8), Chemokine (C-X-C motif) ligand 1, (CXCL1, GROα), Chemokine (C-C motif) ligand 5 (CCL5,RANTES), Monocyte chemoattractant protein-1(MCP-1), Macrophage inflammatory protein 1 α (MIP-1α), Macrophage inflammatory protein 1 β (MIP-1b), Interferon gamma-induced protein 10 (IP-10), Interferon–inducible T Cell Alpha Chemoattractant (I-TAC), Monokine Induced by. Gamma Interferon (MIG), Eotaxin, Thymus and activation-regulated chemokine (TARC), Macrophage-derived chemokine (MDC)- see Figure 5-17).

Antibody	Species	Dilution	Antigen Retrieval	Source
p16	Mouse monoclonal (IgG2A)	1:700	None	Cancer Research UK, Monoclonal antibody laboratory
P21 (WAF-1) (M7202)	Mouse monoclonal (IgG1)	1:10	10 minute microwave in 0.01M sodium citrate	DAKO, Cambridge, UK
Ki67 (MIB-1)	Rabbit polyclonal	1:100	None	Leica Biosystems, Switzerland
Secondary antibody IgG biotin complex	Rabbit anti-mouse	1:300	Applied as secondary layer	DAKO, Cambridge, UK
IgG biotin conjugate	Goat anti-rabbit	1:500	Applied as secondary layer	DAKO, Cambridge, UK
Alexa-Fluor 488	Goat anti mouse	1:150	Applied as secondary layer	Invitrogen Life Technologies, Paisley, UK
Alexa-Fluor 555	Goat anti rabbit	1:150	Applied as secondary layer	Invitrogen Life Technologies, UK
IgG2A negative control	Unimmunized Mouse monoclonal	1:150	None	DAKO, Cambridge, UK
IgG1 negative control	Unimmunized Mouse monoclonal	1:150	None	DAKO, Cambridge, UK
Anti-CCL5 (RANTES) (ab83324)	Rabbit polyclonal	1:50	10 minute microwave in 0.01M sodium citrate	Abcam , Cambridge, UK
Anti-CXCL1 (GROα) (ab86436)	Rabbit polyclonal	1:250	None	Abcam, Cambridge, UK

Table 2-2: Table of antibodies and conditions used for immunohistochemistry.

All reagents were provided by the manufacturer. The plate was supplied coated with pre-optimised antibodies. Each cell line supernatant used was centrifuged at $1x10^3$rpm for 10 minutes and decanted from the cell pellet prior to storage at -20°C. Assay buffer was prepared by the addition of 0.6 ml of 10% bovine serum albumin (BSA) into a final volume of 30 ml with Assay Buffer Stock (provided by manufacturer). After addition of 50µl of the assay buffer to each well, 50µl of supernatant was also added. This was performed in triplicate. The positive control consisted of an antigen mix cocktail provided by the manufacturer, and the negative control consisted of a sample dilution buffer also provided by the manufacturer. The sample was gently tapped for 10 seconds to allow mixing and then allowed to incubate at room temperature for 2 hours. The contents of the wells were then decanted and the wells were then washed using the supplied Wash Buffer (details confidential according to manufacturer). The plate was gently shaken to mix and the contents decanted- this was repeated three times.

100µl of detection antibody was then added to each well. After gentle tapping to mix, the plate was incubated for 1 hour at room temperature. 100 µl of avidin-HRP was mixed with Assay Buffer at a 1:1 ratio by volume, was then added to each well and then incubated for 30 minutes in the dark. The plate was washed with Wash Buffer a further four times and 100 µl development solution added to each well with a subsequent 15 minute incubation in the dark. 100 µl of the supplied stop solution was then added. Absorbance was read at 450nm and 570nm to allow for correction for optical imperfections in the plate within 30 minutes of stopping the reaction.

2.4.3 Fluorescence activated cell sorting (FACS)

Cell transfected with *pBabe-puro*-IRES-EGFP (developed in section 2.3.2) were harvested as described above. Cells were washed by centrifugation at 400xg at 4°C for 5 minutes in ice cold FACS buffer (1X PBS, 1% FCS, 0.02% NaNH3 and 5 mM EDTA), They were then placed in polystyrene tubes (BD Falcon, UK),diluted in ice cold PBS and kept on ice. Subsequently samples were processed on a BD LSRII Flow cytometer (BD Biosciences, Oxford, UK). Analysis was performed using FACSDiva software v 6.1.3 (BD Biosciences, UK).

2.5 Nucleotide analysis methods

2.5.1 Polymerase chain reaction (PCR):

A nested PCR protocol was followed throughout the thesis. Reagent concentrations and thermocycler conditions had been previously optimised in the lab (see Appendix 1). A 23µl PCR reaction mixture was prepared per PCR reaction, containing 0.4µmol of first round forward and reverse gene-specific primers (see Appendix 1) for *CDKN2A* and *TP53*,1-2mM $MgCl_2$ (Qiagen, Crawley, UK), 0.2mM of each dNTP (Life Science, Buckinghamshire, U.K), Q solution (Qiagen, UK) and 1unit of Taq polymerase (Qiagen, UK).2µl of extracted DNA was added to each well of a 96 well plate (Abgene,Epsom,UK) and the reaction mixture then added to each well so that every reaction contained a 25 µl total volume. The plates were then sealed with Thermowell sealers (Corning, Ewloe, Flintshire). The first round PCR was prepared in an Omni PCR UV hood (Bioquell, Berkshire, U.K.) to reduce contamination and then subjected to 37 cycles of denaturing, annealing and extension on a Tetrad

thermocycler (MJ Research, Waltham, MA). 2µl of first round PCR product was then subjected to a second round of PCR using the same reagents as the first round PCR. Reagent concentrations for $MgCl_2$ (Qiagen, Crawley, UK)and Q solution (Qiagen, UK)and thermocycler conditions had also already been optimised for specific second round primers (Appendix 1).The other reagents used in the first round PCR reaction were used at the same concentration in the second round reaction and the 96 well plate was prepared without the Omni PCR UV hood (Bioquell, Berkshire, U.K.) on ice prior to it being placed in the thermocycler.

Number of cycles	Step	Temperature(°C)	Time (minutes)
1	Denaturation	95	4
35	Denaturation	94	1
	Primer annealing	55 or 60	1
	Extension	72	1
1	Final extension	72	10

Table 2-3: PCR reaction conditions for first and second round PCR for CDKN2A and TP53

2.5.1.1 Gel electrophoresis of PCR product

1.5% agarose gels were prepared by addition of 3g of agarose (Sigma-Aldrich, UK) to 150ml of 1 X Tris/Borate/EDTA (TBE)solution (National Diagnostics, Atlanta, GA) then microwaving for 2 minutes until melted. This was then cooled until starting to become viscous. 15µL of Gelred fluorescent nucleic acid dye (Biotum, California) was then added and the gel allowed to set with combs placed within the gel to form wells. Once set, the gel was loaded into the electrophoresis tank (Takara Bio, Kyoto, Japan).5µl of HyperLadder IV (Bioline, London, UK) was added to the furthest left well for each row of wells to provide molecular weight markers. For the rest of the wells, a mix of 2 µl loading buffer (0.25% w/v bromophenol blue, 0.25% w/v xylene

cyanol, 30% v/v glycerol) with 5µl DNA was added to each well. The samples were run for 35 minutes at 135V, visualised using a UV transilluminator (wavelength 294 nm) and photographed.

2.5.1.2 PCR sequencing

Prior to sequencing, PCR reactions were cleaned by ExoSAP-IT(Affymetrix, Santa Clara, CA). This consists of recombinant exonuclease I and shrimp alkaline phosphatase (*Pandalus borealis*) in a buffered solution.2 µl of ExoSAP-IT was added to 5 µl of second round PCR product on ice and subjected to 37^{o}C for 15 minutes followed by 80^{o}Cfor 15 minutes on a thermocyclerApplied Biosystems 7500 (Applied Biosystems, UK).The treated products were then diluted with distilled water (10-20 µl) depending on the intensity of DNA bands on the 1.5% agarose gel from the second round product.

PCR products were then subjected to Sanger sequencing reaction. Each sequencing reaction contains 4 µl of diluted ExoSAP-IT (Affymetrix, CA) product, 1 µlof primer (forward or reverse), 5 µlof distilled water, and 10 µlof Big Dye Terminator (Applied Biosystems, Foster City, CA). The sequencing reaction was run on an ABI 3100 DNA sequencer (Life Science, CA). The sequences obtained were compared with the Catalogue of Somatic Mutations in Cancer (http://www.sanger.ac.uk/genetics/CGP/cosmic) database. Each mutated sample was repeated from the original DNA for mutation confirmation. Polymorphisms were eliminated by comparing their sequence against that held in the Ensembl database (http://www.ensembl.org) and by sequencing non-epithelial tissue (muscle) laser captured from the same patient's sample.

2.5.2 RNA related methods

2.5.2.1 Total RNA extraction

Total RNA was prepared for all applications using the RNeasy RNA minikit as directed by the manufacturers (Qiagen, UK). RNAZap (Invitrogen, Life Science Technology, UK) was applied to all surfaces and equipment. Once cell culture medium had been completely aspirated, cells were lysed directly from culture plates by addition of buffer RLT to which 10 µl β-mercaptoethanol/ml of RLT had been added. The lysate was then pipetted into an eppendorf and vortexed to ensure proper mixing. Homogenisation of the lysate was achieved by pipetting the lysate through a blunt 20G needle fitted to a RNA free syringe. One volume of 70% ethanol was then added to the lysate and mixed by pipetting. The sample was then placed in a spin column within a 2ml collection tip and centrifuged for 15 seconds at $1x10^5$ rpm. The flow through was discarded and 700µl of RW1 was added to the spin column and again centrifuged for 15 seconds at $1x10^5$rpm; the flow through was again discarded. Buffer RLT and Buffer RW1 both contain guanidine salts which immediately inactivate RNases. Having added 500µl of the mild washing buffer RPE to the spin column and again centrifuging for 15 seconds at $1x10^5$rpm and discarding the flow through, a further 500µl Buffer RPE was added and centrifuged at $1x10^5$rpm for 2 minutes. The flow through was again discarded and the spin column was placed in a new collection tube. To this 30-50µl of RNase-free water was added to the spin column membrane; the column was then centrifuged for 1 minute at 10,000 rpm to elute the RNA.

2.5.2.2 Determination of RNA quality and concentration

The RNA concentration was analysed using the Nanodrop ND-1000 spectrophotometer (Thermo Fisher Scientific, UK). The degradation level was assessed using the Agilent 2100 Bioanalyser (Agilent Technologies, Santa Clara, CA). This is a chip-based capillary electrophoresis machine which measures degradation of RNA, DNA and proteins prior to performing RT-PCR and derives a RNA Integrity Number between 0-10 to demonstrate how intact the sampled RNA is. RNA integrity level scores >7 were considered acceptable for further analysis.

2.5.2.3 Microarray analysis of irradiated OE33 cells

RNA was isolated as previously described, from irradiated and unirradiated OE33 cells which had been cultured in triplicate in 6 well plates. Prior to analysis the cells were stored at -20°C. Whole transcript levels were assessed using theHumanHT-12 v4 Expression BeadChip (Illumina, San Diego ,CA) and performed by Dr Charles Mein (Genome Centre, Barts Cancer Institute, Charterhouse Square, London)**.** This involves a first and second strand reverse transcription step. Subsequently an *in vitro* transcription amplification step incorporates biotin labelled nucleotides. The final step involves array hybridization, washing, blocking and streptavidin-Cy3 staining with the results read onto a BeadArray Reader (Illumina, CA).

Results were analysed using Genome Studio 2011 v2011.1 (Illumina, CA). The results are expressed as an increase or decrease in fold change expression relative to the control which was the unirradiated OE33 cells. A fold change of <>2 was taken for further statistical analysis using a t-statistic which was then corrected for multiple testing using a Bonferroni correction with a p value of <0.05 as significant.

To ascertain RNA levels of proteins that were likely to be secreted extracellularly, cellular component ontology of significantly upregulated RNA was undertaken using Genego using the term 'extracellular space': GO:0005615 (Thomson Reuters, NY). This term is defined as 'gene products from multicellular organisms which are secreted from a cell but retained within the organism' (http://www.ebi.ac.uk/QuickGO/GTerm?id= GO:0005576) Suggested genes were then entered into the STRING (Search Tool for the Retrieval of Interacting Genes/Proteins) database (http://string-db.org/) which is a database of known protein-protein interactions. The database was queried to provide a list of protein interactions based on the inputted data which is performed by scoring raw network data for all interaction partners with values listed in descending order**.**

2.5.2.4 Quantitative reverse transcriptase polymerase chain reaction (qRT-PCR) of irradiated cell lines

2.5.2.4.1 Complementary DNA synthesis

First strand cDNA was synthesised using Superscript III reverse transcriptase (Invitrogen Life Technologies, UK). 250ng total RNA (per sample) was added to 1 µl of random primers and 1 µl of 10mM dNTP mix(Invitrogen Life Technologies, UK). The volume was made up to 10 µl with diethylpyrocarbonate treated water. The cDNA mix was prepared (pre reaction) by the addition of 10X RT buffer, 4 µl of 25mM $MgCl_2$, 2µl of 0.1M Dithiothreitol (DTT), 1µl RNaseOUT (40 U/µl) and 1µl of Superscript III reverse transcriptase (all supplied by Invitrogen Life Technologies, UK) to give a final volume of 20 µl.

The sample was mixed gently and briefly centrifuged. Using anApplied Biosystems 7500 thermocycler (Applied Biosystems, UK) the sample was then incubated for 10 minutes at 25°C followed by 50 minutes at 50°C; the reaction was then terminated at 85°C for 5 minutes and chilled on ice. After a further brief centrifugation, 1 µl of RNase H was added to each tube to remove the RNA template from the cDNA:RNA hybrid and incubated for 20 minutes at 37°C. The resulting cDNA was stored at-20°C until required. Control RNA was provided by the manufacturer to act as a positive control, and H_2O acted as a negative control.

2.5.2.4.2 qRT-PCR reaction preparation

Prepared cDNA and Taqman gene expression assays (Invitrogen Life Technologies, UK) were thawed on ice, gently vortexed and centrifuged. The reactions were prepared in triplicate, with each reaction being prepared in 20µl total reaction volume consisting of 20x TaqMan® Gene Expression Assay (Invitrogen Life Technologies, UK), 2x TaqMan® Gene Expression Master Mix (Invitrogen Life Technologies, UK), cDNA template (at 2ng/µl) and RNase-free water (Qiagen, UK) . The reactions were run on an Applied Biosystems 7500 thermocycler (Applied Biosystems, UK) with the following thermal cycling conditions: 50°C for 2minutes, 95°C for 10 minutes, cycle at 95°C for 15 seconds, then 40 cycles at 60°C for 1 minute.

2.5.2.4.3 qRT-PCR gene expression analysis

All reactions were performed in triplicate and the reactions repeated on two occasions. All genes were normalised using the house keeping gene GAPDH (glyceraldehyde 3-phosphate dehydrogenase; Hs02758991_g1 reference sequence: NM_001256799.1), UBC (ubiquitin C; Hs00824723_m1 reference sequence: NM_021009.5), ACTB (β-actin ; Hs03023943_g1 reference sequence: NM_001101.3), E1f-α2 (initiation factor α2; Hs00426773_gH) between samples in each set, so that the relative expression of genes of interest could be established. Unirradiated OE33 cells were used as the control in each experiment**.** The delta delta CT (ΔΔCT) method (Livak & Schmittgen 2001) was used to ascertain the relative expression level of each gene as follows:

1. ΔCT was calculated by subtracting the average gene CT value from the average housekeeping CT value.

2. ΔCT values from each sample was subtracted from the reference sample to yield a ΔΔCT value (ΔΔCT = ΔCTirradiated_Cells – ΔCTunirradiated_Cells) and relative gene expression values $2^{(\text{-log fold values})}$ were calculated using the following equation – $2^{-\Delta\Delta CT}$.

The results were analysed using a Mann Whitney test on fold changes relative to the control sample.

2.6 Statistics

GraphPad Prism® 5 programme was used for all statistical analysis. Error bars represent standard error of the mean unless otherwise stated. All statistical analyses are explained in further detail in the relevant section.

2.6.1.1 Statistical tests for assessment of immunohistochemistry of p21 and p16 expression and for Ki67/p16 and Ki67/p21 co-expression

χ-squared test (section 5.3.1&5.3.2).

2.6.1.2 Statistical test to measure cell viability of irradiated OE33 cells

2 way ANOVA with Bonferroni post hoc testing (section 5.3.3).

2.6.1.3 Statistical test for assessment of SA β-Galactosidase expression in irradiated OE33 cells and OE33 cells exposed to H_2O_2.

Kruskal Wallis with Dunn's post-test (section 5.3.3.1&5.3.4).

2.6.1.4 Statistical test for MTT assay to assess proliferation in OE33 cells irradiated at 2Gy and 10Gy

2 way unrelated ANOVA with Bonferroni post hoc testing (section 5.3.3.2).

2.6.1.5 Statistical test for colony formation assay of irradiated OE33 cells

2 way unrelated ANOVA with Bonferroni post hoc testing (section 5.3.3.3).

2.6.1.6 Statistical test to assess proliferation by admixture of senescent and non-senescent OE33 cells.

Kruskal-Wallis with Dunn post testing (section 5.3.5.1).

2.6.1.7 Statistical test to assess response of unirradiated OE33 cells to conditioned media

Mann Whitney-test (section 5.3.5.2).

2.6.1.8 Statistical test for gene expression microarrays

Student's t-test with Bonferroni correction (section 5.3.6).

2.6.1.9 Statistical test to assess qRT-PCR results.

Mann Whitney test (section 5.3.6).

2.6.1.10 Statistical test for ELISA

Mann-Whitney test (section 5.3.6).

2.6.1.11 Statistical test to assess the effect of recombinant protein on OE33 cell proliferation as measured by MTT assay

Goodness of fit and nonlinear regression analysis (section 5.3.7).

2.6.1.12 Statistical test for assessment of CCL5 and CXCL1 immunohistochemistry in ex-vivo tissue specimens.

2 way ANOVA with Bonferroni post hoc correction (section 5.3.8).

Chapter 3 Clonal selection after endoscopic therapy of Barrett's related high grade dysplasia and adenocarcinoma.

3.1 Introduction

BO represents a form of field cancerization. This is defined as a preconditioning of an area or multiple areas of epithelium to tumour growth as a result of a clonal proliferation of mutant cells through the epithelium without causing neoplasias (Graham TA*et al.*2011).Longitudinal studies of patients with Barrett's oesophagus initially suggested clonal progression of a single clonal population from a single ancestral crypt to adenocarcinoma (M T Barrett *et al.* 1999). However, recent work has demonstrated that a field such as BO may in fact contain several clonal populations (Leedham *et al.* 2008)and that genetic diversity *per se* is a risk factor for progression to OAC (Maley *et al.* 2006) suggesting that interaction between clonal populations may drive OAC development.

Several forms of endoscopic ablation therapy exist to treat Barrett's dysplasia (see section 1.8.1). The most recent and most successful is RFA which involves the delivery of a thermal injury to areas of Barrett's mucosa(Pouw *et al.* 2008). 1 year

follow up data of patients undergoing this therapy has demonstrated eradication to squamous mucosa from IMC and HGD of 80% (Ganz *et al.* 2008), although it is becoming apparent that with longer follow up, patients can increasingly suffer from recurrent high and lowgrade dysplasia (Shaheen *et al.* 2011). Endoscopic mucosal resection, in which the tissue is removed endoscopically rather than being destroyed, is often used in combination with RFA particularly for nodular disease(Haidry *et al.* 2013).

The cause of persistent and recurrent high grade dysplasia and intramucosal cancer is likely to be related to the presence of a persistent cellular origin of Barrett's mucosa. Therefore studying the source of cells carrying persistent protumorigenic mutations before and after ablation therapy may give insight as to the source of regenerating Barrett's mucosa. The theoretical sources include cells with protumorigenic mutations persisting in squamous and non-dysplastic Barrett's mucosa, the same cells being present in submucosal glands or their associated ducts or cells being present in buried Barrett's- Barrett's tissue located beneath normal squamous tissue (discussed in section 1.8.2.3).Understanding this may also answer why Barrett's mucosa is difficult to eradicate using RFA in a significant minority of patients. Furthermore it may also give insight as to why patients develop recurrent dysplasia if they are eradicated to Barrett's mucosa.

Most work on understanding clonal progression in Barrett's oesophagus has been done in patients progressing to adenocarcinoma who have not undergone any endoscopic therapy.(Wong, Paulson, L J Prevo, et al. 2001; Barrett et al. 1999). No longitudinal study has assessed clonal progression in patients before and after

therapy for Barrett's related HGD and OAC in patients in which these pathologies are persistent or recurrent. An investigation of the clonality of Barrett's oesophagus before and after treatment enables us to infer how therapy may alter the clonal landscape in Barrett's oesophagus.

3.2 Aims

a) To examine a longitudinal case series of patients who have undergone RFA and EMR and understand the clonal correlates of persistent or recurrent HGD or OAC in patients undergoing endoscopic therapy.

b) To establish the potential reasons why clonal cancer-associated cell populations may be persistent despite treatment with ablation therapy.

c) To establish the potential reasons why clonal cancer associated cell populations may recur after treatment with ablation therapy.

3.3 Methods

Approval for the study was obtained from National Research Ethics Service Committee London Stanmore (Ref: 11/LO/1613).Patient records stored in the UK National RFA database from 2007 to present were consulted. All patients had undergone therapy according to their clinical need. Biopsies were largely taken according to guidelines for Barrett's surveillance which stipulates quadrantic biopsies every two centimetres in the affected segment (British Society of Gastroenterology 2005 guidelines (www.bsg.org.uk). All tissue was assessed by two independent pathologists (Professor Sir Nicholas Wright, Dr Manuel Rodriguez-Justo) for Barrett's

metaplasia, dysplasia and adenocarcinoma according to British Society of Gastroenterology 2005 guidelines (www.bsg.org.uk). Only patients with recurrent or persistent disease after RFA and/or endoscopic mucosal resection (EMR) of HGD or intramucosal adenocarcinoma (IMC) were chosen for analysis. Furthermore, patients had to haveundergone two further endoscopic samplings subsequent to the initial ablation therapy.Persistent disease was defined as no down staging of the original IMC or HGD to non-dysplastic Barrett's mucosa. Recurrent disease was defined as HGD or IMC development after successful endoscopic therapy with down staging to non-dysplastic Barrett's mucosa.Furthermore, patients had to have undergone two further endoscopic samplings subsequent to the initial ablation therapy to be included in this study. All paraffin embedded blocks available for each patient for the entire therapeutic time line were obtained (total number of FFPE samples: 186, number of patients= 19).

Sections containing the original pathology for each patient underwent macrodissection and nested PCR sequencing for somatic mutations commonly associated with the Barrett's metaplasia-dysplasia-cancer sequence (*CDKN2A exon 2*, *TP53* (exons 5-8)). If the specimen contained a detectable mutation, further blocks along the patient's treatment timeline underwent further mutational analysis of all of the original target genes. Initial screening for somatic mutations was performed by cutting six serial sections at 6 µm thickness onto normal glass slides. This tissue was dewaxed and needle scraped into 30µL digestion buffer (Arcturus Bioscience, Mt View, CA). Negative control tubes containing 30 µl Pico Pure proteinase K solution (Invitrogen Life Technologies, UK) solution and no needle scraped material were included. Tubes were then centrifuged at 4.5x*g* for 1 minute and incubated at

65°Covernight. A 10 minute incubation at 95°C denatured the proteinase K (Invitrogen Life Technologies, UK)and the lysate was then stored at -20°C.

3.3.1 Laser capture microdissection

All cancers containing detectable mutations underwent laser capture microdissection where possible. This technique is well described (Leedham *et al.* 2008). As described in section 2.2.4, H&E slides of the paraffin embedded cancer were prepared. These were serial to further sections prepared on laser capture slides (P.A.L.M. Microlaser technologies, Germany). Once suitable areas for dissection had been determined from the H&E, the laser capture microdissection slides(P.A.L.M. Microlaser technologies, Germany) were stained with methylene green (Sigma-Aldrich, UK) for 2 minutesand microdissected on a dedicated laser capture microscope (P.A.L.M. Microlaser technologies, Germany). The epithelium was catapulted into eppendorf adhesive caps (P.A.L.M.Microlaser Technologies ,Germany) and digested with 12 µlPico Pure proteinase K solution (Invitrogen Life Technologies, UK). A laser capture tube containing 12 µl Pico Pure proteinase K solution and no laser capture material was also prepared as a negative control. The tubes were centrifuged at 4.5x*g* for 1 minute and then incubated overnight at 65° C. The samples then underwent nested PCR. Muscle distant from the pathology of interest was taken for PCR sequencing of constitutional DNA to exclude polymorphisms.

Once analysed, the sequence results from needle scraping and laser capture were geographically plotted according to where the biopsies were taken from, using the

gastroscopy reports as a guidewhich were anonymised using each specimen's pathology block number.

3.4 Results

3.4.1 Overview of results

Needle scraped tissue sections of 19 patients with recurrent or persistent oesophageal adenocarcinoma or high grade dysplasia underwent nested PCR for *TP53*, exons 5-8, and *CDKN2A*. Of these, 8 (42%) had detectable *CDKN2A* or *TP53*mutations (3 with recurrent disease, 5 with persistent disease) and all available tissue specimens from the patient's treatment time course were obtained. The remainder were uninformative for mutations in these genes. The frequency of mutations in this cohort was similar to those reported in the COSMIC database (http://www.sanger.ac.uk/genetics/CGP/cosmic/).

Of the 5 patients with persistent disease, 3 had one mutation present throughout the disease course (Pt 1, 2 &5). 1 patients had several mutations in different genes detected at various time-points throughout the disease course (Pt 4). Patient 3 had more than one persistent mutation detected. In recurrent disease, one patient had a persistent mutation, 2 patients did not. Overall, 5 patients had more than one mutation detected in all the tissue analysed.The summarised results are shown in

Table 3-1**.**